Title: Differential amplicons for the evaluation of RNA integrity extracted from complex environmental samples

Authors: Fabien Cholet[#], Umer Z. Ijaz & Cindy J. Smith

Infrastructure and Environment Research Division, School of Engineering, University of Glasgow, UK, G12 8LT

Address correspondence to f.cholet.1@research.gla.ac.uk

Abstract

Background

Reliability and reproducibility of transcriptomics-based studies are highly dependent on the integrity of RNA. Microfluidics-based techniques based on ribosomal RNA such as the RNA Integrity Number (RIN) are currently the only approaches to evaluate RNA integrity. However, it is not known if ribosomal RNA reflects the integrity of the meaningful part of the sample, the mRNA. Here we test this assumption and present a new integrity index, the Ratio amplicon, R_{amp}, to monitor mRNA integrity based on the differential amplification of long to short RT-Q-PCR amplicons of the glutamine synthetase A (*glnA*) transcript.

Results

We successfully designed and tested two R_{amp} indexes targeting *glnA* transcripts. We showed in a suite of experimental degradations of RNA extracted from sediment that while the RIN in general did reflect the degradation status of the RNA well the R_{amp} mapped mRNA degradation better as reflected by changes in Reverse Transcriptase Quantitative PCR (RT-Q-PCR) results. Furthermore, we examined the effect of degradation on transcript community structure by amplicon sequencing of the *16S rRNA, amoA* and *glnA* transcript which was successful even form the highly-degraded samples. While RNA degradation changed the community structure of the mRNA profiles, no changes were observed between successively degraded 16S rRNA transcripts profiles.

Conclusion

As demonstrated, transcripts can be quantified and sequenced even from highly degraded samples. Therefore, we strongly recommend that a quality check of RNA is conducted to ensure validity of results. For this both the RIN and R_{amp} are useful, with the R_{amp} better evaluating mRNA integrity in this study.

Key words: RNA; mRNA**;** RNA integrity; RIN; differential amplicons; R_{amp}

Background

A key question in environmental microbiology is to determine the functioning and activity of microbial communities. While genomic approaches have resulted in an unprecedented understanding of their structure and complexity [1], they do not inform of the actual activity and functioning at a given time. In this case targeting the transcriptome, that is the subset of genes that are actively transcribed at a given time, is more informative. While there can be substantial post translational regulation that may prevent final protein synthesis and/or activity, gene expression is the direct link between the genome and the function it encodes and therefore is a stronger link to activity than DNA approaches alone [2]. As a result transcriptomics based approaches are widely used to assess microbial activity and functioning in the environment [3, 4]. The premise is that that messenger RNA (mRNA) turn-over within cells is rapid, ranging from a few minutes to less than an hour [5]. As such a snap-shot of the transcriptome reflects the cells transcriptional response to its surrounding environment and metabolic needs at a given time.

A challenge for all transcript-based studies, not least for those from environmental samples, is to ensure the quality and integrity of the RNA on which the results are based. Extracted RNA is prone to degradation both during the extraction procedure, post-extraction handling and over time. Factors such as RNase activity, physical degradation during extraction procedures, and even storage can degrade RNA. If there is significant post-extraction degradation among different samples that are to be compared, the interpretation of results may be compromised. In other words, differences between samples may arise as a result of post-extraction degradation, as opposed to representing actual difference in gene expression. Indeed, meaningful and reproducible results can only be obtained when working with good quality,

intact RNA, whether it is eukaryotic RNA [6–9] or Prokaryotic RNA [10]. As such an initial quality check of extracted RNA, not least from complex environmental microbial communities should be the essential first step before proceeding to any downstream applications. This quality check would help to ensure that any differences observed between samples are due to actual changes in gene expression rather than differences in samples integrity as a result of degradation.

Current methods to evaluate the integrity of extracted RNA are based on ribosomal RNA (rRNA). These approaches evaluate integrity as a ratio between the 16S and 23S ribosomal RNA: 16S, 23S and 5S rRNA are synthetized as one primary transcript and are separated upon maturation [11]. The 16S and 23S ribosome should therefore be present at a ratio 1:1. However, as the 23S ribosome is approximately twice as large as the 16S ribosome, for intact, non-degraded RNA, the expected ratio of 23S:16S RNA is 2:1. However, the caveat of this approach is the assumption that the integrity of rRNA reflects that of the overall RNA, including mRNA. The relationship between the integrity of rRNA and that of mRNA has not been demonstrated [6]. Indeed, there are several reports indicating the more stable properties of rRNA compared to mRNA [12–14]. As such, the usefulness of this ratio to assess mRNA integrity is still unclear.

In its simplest form, evaluating ribosomal RNA integrity is an electrophoretic separation of RNA in a gel matrix. Essentially, a visual check for the presence of the characteristic bands corresponding to 16S and 23S rRNA. More advanced techniques based on microfluidics are better suited for assessing RNA quality, allowing for the calculation of integrity indexes, such as the RNA Integrity Number, RIN (Agilent Technologies) or the RNA Quality Score, RQI (BioRad). These scores vary between 0 (RNA totally degraded) and 10 (“perfect” RNA). A value of 7 has been suggested as a limit between “good” and “bad” quality RNA extracted from bacterial pure cultures [10]. However, RNA extracted from natural environments such as

soil or sediment will likely have lower quality due to the more complex matrixes and, often, harsh extraction techniques routinely used, such as bead beating [15] but this information is not widely reported in the literature. Nevertheless, as highlighted above, even if reported, a shortcoming for RIN/RQI algorithms is that they are primarily based on rRNA (16S/23S ratio) which may degrade differently from mRNAs; the relevance of such indexes for gene expression analysis is therefore unknown.

In Eukaryotic gene expression studies, an alternative index often used to evaluate the level of mRNA degradation is the 3'-5' ratio [16]. This technique is based on the observation that Eukaryotic mRNAs generally degrade from the 5' to the 3' end, with the 3' poly A tail acting as a protective agent. As a result, Reverse Transcriptase-PCR (RT-PCR) targeting the 5' end of the transcript is less likely to be produce amplicons than those targeting the 3' end. A high 3':5' ratio (low 5' copy number) is therefore an indication of mRNA degradation. This technique cannot be applied to prokaryotic mRNAs as they generally don't possess poly A tails, and when they do, the tail enhances mRNA degradation [17]. Recently, a new approach called differential amplicon (Δamp) has been developed [18]. This technique is based on the differential amplification of RT-PCR amplicons of different lengths from the same mRNA target as a new means to determining RNA integrity (see also [19]). Here it was observed that the copy number of long RT-Q-PCR targets correlated with mRNA degradation whereas the short targets were more stable. Since this approach doesn't rely on the presence of the poly A tail, it could theoretically be adapted to prokaryotic mRNAs. Although this has not been directly observed for prokaryote RNA, Reck *et al* [20] showed a similar response of a exogenous green-fluorescent-protein mRNA(GFP) that they spiked into stool RNA to montior its intergery when subjected to different storage conditions. They showed that the copy number of the spiked exogenous GFP correlated well with RNA integrity when targeting a long amplicon (≥500bp), whereas the short amplicon (≤100bp) remained constant, even in

126 highly degraded RNA preparations. This indicated that, as was observed by Björkman and co-
127 workers, longer mRNA targets reflect degradation better. As such, the difference in RT-Q-
128 PCR performance, reflected by the difference in cycle threshold (Ct) between a short and a
129 long amplicon from the same cDNA target could be used as an index to reflect mRNA
130 integrity.

131 Here, we propose to exploit the differential amplicon approach to develop a ratio of
132 long to short amplicons directly targeting mRNA transcripts of the same target but of
133 differing lengths by RT-Q-PCR as an indicator of overall mRNA integrity. For this we
134 propose the ubiquitous bacterial glutamine synthetase A transcript (*glnA*) as the target.
135 Glutamine synthetase is a ubiquitous gene, found in Bacteria and Archaea [21, 22], with a role
136 in assimilating inorganic nitrogen (ammonia) into amino acids [23]. The *glnA* transcript has
137 been used previously in RT-(Q)-PCR approaches to evaluate RNA extraction yield from soils
138 [24–26]. However, as the expression of *glnA* is regulated by ammonia concentration [27–29],
139 the copy number of this transcript can vary making comparison between studies difficult. Our
140 approach overcomes this difficulty by calculating the ratio of long to short *glnA* transcripts.
141 We designate this the Ratio Amplicon (R_{amp}), and propose it as an indicator of mRNA
142 integrity, independent of absolute gene expression.

143 Specifically, this study aims to design and test the Ratio Amplicon (R_{amp}) approach to
144 evaluate bacterial mRNA integrity extracted from marine sediments. Furthermore, we aim to
145 compare and evaluate this approach against the conventional ribosomal based RNA integrity
146 index, RIN. Comparison between the two approaches was conducted by monitoring how well
147 both indexes reflected experimental RNA degradation (UV, heat, RNase, freeze/thaw). The
148 impact of RNA degradation and the ability of the two indexes to predict ribosomal and
149 mRNA integrity was evaluated via quantification of two commonly surveyed bacterial
150 transcripts, the highly abundant ribosomal 16S rRNA and mRNA from the less abundant

bacterial ammonia monooxygenase (*amoA*). Finally, the effect of RNA degradation on transcript community structure was evaluated by amplicon sequencing of the cDNA obtained from sequentially degraded samples.

We hypothesised that i) the R_{amp} would be a better predictor of mRNA integrity than the RIN and ii) RNA degradation would adversely affect both transcript quantification and community composition.

Methods

Sediment Samples

Surface mud samples (0 to 2 cm) were collected on 11/01/2017 from Rusheen Bay, Ireland (53.2589° N, 9.1203° W) (presence of *amoA* genes/transcripts previously established [30, 31] in sterile 50ml Eppendorf tubes, flash frozen and stored at -80°C until subsequent use.

Design of new *glnA* primers

To design new primers, bacterial *glnA* sequences were downloaded from the GeneBank database [32]. Sequences related to environmental bacteria were subjected to BLAST search [33] in order to gather additional sequences. In total eighty-four sequences (Additional file 1) were aligned using MUSCLE [34] and a phylogenetic neighbour joining tree was drawn in MEGA 7 [35]. Based on sequence similarity, eight groups could be distinguished (see Additional file 4: Figure S1). Primer sequences from Hurt and co-workers [15] were aligned in each individual group to determine coverage and new primers (Table 1) were designed based on conserved regions to target the same groups with varying length primers.

Primers were tested on DNA and cDNA using environmental DNA/RNA extractions and environmental cDNA, as template. *glnA* genes were amplified (BIOTAQ DNA polymerase kit; Bioline) in a 25µl final volume composed of 2.5µl BioTaq10x buffer, 18µl water, 1.5µl

176 $MgCl_2$ (50mM), 0.5µl of each primer (10µM), 0.5µl dNTPs (10µM each), 0.5µl *Taq* DNA
177 polymerase and 1µl of template. PCR conditions were as follow: 95°C 5 min, (94°C 30 sec,
178 60°C 30 sec, 72°C 30 sec) x 30 and 72°C 5 min.
179
180 **RNA preparation from sediment**
181 All surfaces and equipment were cleaned with 70% ethanol and RNase Zap (Ambion) before
182 sample processing. All glassware and stirrers used for solutions preparation were baked at
183 180°C overnight to inactivate RNases. All plasticware was soaked overnight in RNase away
184 (ThermoFisher Scientific) solution. Consumables used, including tubes and pipet tips were
185 RNase free. All solutions were prepared using Diethylpyrocarbonate (DEPC) treated Milli-Q
186 water. A simultaneous DNA/RNA extraction method, based on that of Griffiths and co-
187 workers [36] was used to recover nucleic acids from sediment. Briefly, 0.5g of sediments
188 were extracted from using bead beating lysing tubes (Matrix tube E; MP Biomedical) and
189 homogeneised in 0.5ml CTAB/phosphate buffer (composition for 120 ml: 2.58g
190 $K_2HPO_4.3H_2O$; 0.10g KH_2PO_4; 5.0g CTAB; 2.05g NaCl) plus 0.5ml
191 Phenol:Chlorophorm:Isoamyl alcohol (25:24:1 v:v:v). Lysis was carried out on a FastPrep
192 system (MP Biomedical) (S: 6.0; 40sec) followed by a centrifugation at 12,000g for 20min
193 (4°C). The top aqueous layer was transferred in a fresh 1.5ml tube and mixed with 0.5ml
194 chlorophorm:isoamyl alcohol (24:1 v:v). The mixture was centrifuged at 16,000g for 5min
195 (4°C) and the top aqueous layer was transferred in a new 1.5ml tube. Nucleic acids were
196 precipitated by adding two volumes of a solution containing 30% $poly(etlyleneglycol)_{6000}$
197 (PEG6000) and 1.6M NaCl for 2 hours on ice and recovered by centrifugation at 16,000 x g
198 for 30 min (4°C). The pellet was washed with 1ml ice-cold 70% ethanol and centrifuged at
199 16,000g for 30 min (4°C). Ethanol wash was discarded and the pellet was air dried. Once the

ethanol was completely evaporated, the pellet was re-suspended in DEPC treated water. DNA/RNA preparations were stored at -80°C if not used immediately.

RNA was prepared from the DNA/RNA co-extraction by DNase treating with Turbo DNase Kit (Ambion) using the extended protocol: half the recommended DNase volume is added to the sample and incubated for 30min at 37°C, afterwhich the second half of DNase is then added and the sample is re-incubated at 37°C for 1 hour. Success of the DNase treatment was checked by no PCR amplification of the V1-V3 Bacterial *16S rRNA* gene [4].

RNA degradation experiments

Physical degradation

To obtain RNA with controlled degradation status, DNA free RNA preparations (≈8µl) were aliquoted from an initial extraction in separate 0.2ml RNase free tubes and incubated at 90°C or under a UV lamp for 0, 10, 45 or 90 minutes. To determine the potential effect of repeated freeze-thaw on RNA preparations, the same 15µl DNA-free RNA was exposed to cycles of freezing (at -80°) and thawing (on ice) as follows - 0, 1, 3, 5, 7 and 10 freeze-thaw cycles. cDNA was then generated for each individual aliquot as described later.

Enzymatic Degradation by RNase I

For RNAse I degradation experiment, 40µl aliquots of DNA-free RNA was incubated at 37°C for 40min in the presence of increasing concentrations of RNaseI (supplier): 0 (buffer only), 2, 10, 20 and 40 Units RNase I/ µg RNA. The reaction was stopped by adding 10µl β-mercaptoethanol and RNA was recovered by ethanol precipitation: 5µl of 7.5M ammonium acetate and 137.5µl 100% ethanol was added and the mixture was precipitated overnight at -20°C. RNA was pelleted by centrifugation 16,000 x g for 40min at 4°C and the pellet was washed with 480µl ice cold 70% ethanol and pelleted by centrifugation at 16,000g for 30min

at 4°C. The pellet was air dried and re-suspended in 40µl of DEPC-treated water. An aliquot of RNA that did not undergo ethanol precipitation was also included for comparison (designated NT: "Not Treated").

Reverse Transcriptase Reaction

DNA-free RNA was used for *glnA* cDNA synthesis using Superscript III kit (Invitrogen) and gene specific priming. The initial RT mixture containing 3µl water, 1µl reverse primer GS1_new (10µM), 1µl dNTP's (10mM each) and 5µl template was incubated at 65°C for 5 min and quickly transferred on ice for 1 min. A second mix composed of 4 µl 5X first-strand buffer, 1 µl 0.1 mM dithiothreitol (DTT), and 1µl SuperScript III (200 units/µl) was added and the resulting mixture was incubated at 55°C for 50 min and then at 72°C for 15 min. The primers and PCR conditions for the amplification of *glnA* targets from cDNA were similar to those used for DNA.

For *16S rRNA* and *amoA* genes, Superscript III kit (Invitrogen) and random hexamers priming was used. The initial RT mixture containing 3µl water, 1µl random hexamer (50µM), 1µl dNTP's (10mM each) and 5µl template was incubated at 65°C for 5 min and quickly transferred to ice for 1 min. A second mix composed of 4 µl 5X first-strand buffer, 1 µl 0.1 mM dithiothreitol (DTT), and 1µl SuperScript III (200 units/µl) and 1µl RNase inhibitor (40U/µl) was added and the resulting mixture was incubated at 25°C for 5 min, 55°C for 50 min and then at 72°C for 15 min.

RNA integrity evaluation

RNA integrity number

RINs were determined at all degradation points, using the automated 2100 Bioanalyser platform (Agilent Technologies) with the Prokaryote total RNA Nano chip, following the manufacturer's instructions.

glnA Q-PCR and Ratio amp (R_{amp}) calculation

glnA cDNA underwent Q-PCR, to amplify varying length amplicon fragments with primer combination as detailed in table 1). Three *glnA* amplicons were produced (Fig. 1), a 120bp amplicon (amplicon 1) generated using the primer pair GS1_new/GSFw1200, a 170bp amplicon (amplicon 2) generated using the primer pair GS1_new/GS2_new and a 380bp amplicon (amplicon 3) generated using the primer pair GS1_new/GSFw900. Q-PCR reaction (10µl) was composed of 5µl EVAGreen Supermixes (SsoFast; Bio-Rad), 0.3µl of each primers (10µM) and 1µl of cDNA template (1/10 diluted). The Q-PCR condition was as follows: 95°C-30sec, (95°C-10sec; 65°C-10 sec) x 35 cycles; plate read at 65°C. Melt curve analysis was performed from 65°C to 95°C with 0.5°C increment every 5 sec.

The Ct value of each assay was recorded and the differential amplicon ratios (R_{amp}) were calculated for each degradation point as follows:

$$R_{amp} = \frac{35 - Ct(long\ amplicon)}{35 - Ct(short\ amplicon)}$$

The value of 35 was chosen as the maximum number of Q-PCR cycles the reaction underwent. A transformation of the differential amplicon was applied in order to have a theoretical maximal value of 1 (no degradation of RNA) and a theoretical minimal value close to 0 (totally degraded RNA).

amoA and _16S rRNA_ RT-Q-PCR

For all degradation experiments, the Cts of the Bacterial *amoA* and the Bacterial *16S rRNA* was determined by Q-PCR of the cDNA preparations. The *amoA* Q-PCR was carried out in a

20µl reaction volume composed of 10µl 5µl EVAGreen Supermixes (SsoFast; Bio-Rad), 0.4µl of each primer (BacamoA-1F and BacamoA-2R) (10µM each), 7.2µl water and 2µl of cDNA template (1/10 diluted). The Q-PCR cycle was as follows: 95°C-5 min, (95°C-30sec, 47°C-30 sec, 72°C-1min, 81°C-1sec→ plate read) x 40 cycles. Melt curve analysis was performed from 65°C to 95°C with 0.5°C increment every 5 sec. *16S rRNA* cDNA targets were quantified in a 20µl reaction volume composed of 10µl Itaq Universal Probes Supermix (Bio-Rad), 1.8µl each primer (1369F and 1492r) (10µM each), 0.4µl probe (1389P) (10µM), 5µl water and 1µl cDNA template (1/10 diluted). The Q-PCR cycle was as follows: 95°C-10min, (95°C-10sec, 60°C-30sec) x 40 cycles and 40°C-10min. All primers are detailed in table 1.

Illumina sequencing

The qualitative effect of RNA degradation the community composition of the three bacterial genes (*amoA*, *glnA* and 16S rRNA) was determined by sequencing the amplicons generated from the cDNA preparations obtained after RNAse I degradation. For each PCR amplification was carried out using the HotStartTaq PCR kit (Qiagen) in the following mix 25µl volume: 19.8µl water, 0.5µl of each primer (10µM each), 0.5µl dNTPs (10µM each), 0.2µl HotStartTaq, 2.5µl of 10x PCR buffer and 1µl cDNA template (10^{-1} and 10^{-3} diluted for functional genes and 16S rRNA respectively). Primers used for sequencing are listed in table 1 (Illumina adaptors were added at the 5' end of the sequencing primers for PCR: 5'-TCG TCG GCA GCG TCA GAT GTG TAT AAG AGA CAG (forward adaptor); 5'-GTC TCG TGG GCT CGG AGA TGT GTA TAA GAG ACA G (reverse adaptor). The PCR cycles were as follows: *amoA*: 95°C-15min, (94°C-30sec, 55°C-30sec, 72°C-30sec) x 32 cycles and 72°C-10min final extension; *glnA*: 95°C-15min, (94°C-30sec, 55.6°C-40sec, 72°C-40sec) x 32 cycles and 72°C-7min final extension; 16S rRNA: 95°C-15min, (94°C-45sec, 50°C-30sec,

298 72°C-40sec) x 25 cycles and 72°C-10min final extension. For each functional gene, three
299 separate PCRs were carried out, using the same conditions, and pooled together for further
300 processing.
301 PCR amplicons were cleaned using the AMPure XP beads kit following the manufacturer's
302 recommendations. Illumina indexes were then attached using the Nextera XT Index Kit with
303 the following PCR condition: 95°C-15min, (95°C-30sec, 55°C-30sec, 72°C-30sec) x 8 cycles
304 and 72°C-5min. The resulting amplicons were purified using the AMPure XP beads kit and
305 eluted in 25µl water. After this step, some preparations were randomly chosen (2 per genes)
306 and run on the Bioanalyser following the DNA 1000 Assay protocol (Agilent Technologies)
307 to determine the average length of the amplicons and to check for the presence of unspecific
308 products. Finally, DNA concentration was determined using fluorometric quantification
309 method (Qubit) and molarity was calculated using the following equation:
310 (concentration in ng/µl) × 10^6 = (660 g/mol × average library size).
311 Libraries were pooled in equimolar amount, and checked again on the Bioanalyser and the
312 final library was sent to the Earlham Institute (Norwich Research Park, Norwich, UK) for
313 Illumina MiSeq amplicon sequencing.
314
315 **Bioinformatics**
316 *Construction of the reference databases*
317 The following sequences were downloaded (see Additional file 2): *amoA* sequences from
318 Fungene (http://fungene.cme.msu.edu/) alongside NCBI sequences (n=642); and bacterial
319 *glnA* sequences (n=1330) as FASTA files from Microbial Genome Database
320 (http://mbgd.genome.ad.jp). For *amoA* sequences, the NCBI taxonomy was given in the
321 FASTA headers whereas for *glnA* sequences, the MBGD Archive
322 (http://mbgd.genome.ad.jp/htbin/view_arch.cgi) was used to download annotations

(mbgd_2016_01) associated with the sequences, and a custom script was written to identify and tag the sequences with NCBI taxonomy. Subsequently, R's rentrez [37] package was used to get taxonomic information at different levels to generate a taxonomy file for *glnA* sequences. The FASTA file and the corresponding taxonomy file was then formatted to work with Qiime. For *16S rRNA* we used the SILVA SSU Ref NR database release v123.

Processing of amplicon sequences

Abundance tables were obtained by constructing operational taxonomic units (OTUs) as follows. Paired-end reads were trimmed and filtered using Sickle v1.200 [38] by applying a sliding window approach and trimming regions where the average base quality drops below 20. Following this we apply a 10 bp length threshold to discard reads that fall below this length. We then used BayesHammer [39] from the Spades v2.5.0 assembler to error correct the paired-end reads followed by pandaseq v(2.4) with a minimum overlap of 20 bp to assemble the forward and reverse reads into a single sequence. The above choice of software was as a result of author's recent work [40, 41] where it was shown that the above strategy of read trimming followed by error correction and overlapping reads reduces the substitution rates significantly. After having obtained the consensus sequences from each sample, the VSEARCH (v2.3.4) pipeline (all these steps are documented in https://github.com/torognes/vsearch/wiki/VSEARCH-pipeline) was used for OTU construction. The approach is as follows: the reads are pooled from different samples together and barcodes added to keep an account of the samples these reads originate from. Reads are then de-replicated and sorted by decreasing abundance and singletons discarded. In the next step, the reads are clustered based on 97% similarity, followed by removing clusters that have chimeric models built from more abundant reads (--uchime_denovo option in vsearch). A few chimeras may be missed, especially if they have parents that are absent from

the reads or are present with very low abundance. Therefore, in the next step, we use a reference-based chimera filtering step (--uchime_ref option in vsearch) using a gold database (https://www.mothur.org/w/images/f/f1/Silva.gold.bacteria.zip) for *16S rRNA* sequences, and the above created reference databases for *glnA* and *amoA* genes. The original barcoded reads were matched against clean OTUs with 97% similarity to generate OTU tables (4108, 1691, and 55 OTU sequences for 16SrRNA, *glnA* and *amoA* respectively). The representative OTUs were then taxonomically classified using assign_taxonomy.py script from Qiime [42] against the reference databases. To find the phylogenetic distances between OTUs, we first multi sequence aligned the OTUs against each other using Mafft [43] and then used FastTree v2.1.7 [44] to generate the phylogenetic tree in NEWICK format. Finally, make_otu_table.py from Qiime workflow was employed to combine abundance table with taxonomy information to generate biome file for OTUs.

Statistical analysis

All statistical analyses were carried out in R. For degradation experiments RIN and R_{amp} values were compared between time points with one-way ANOVA, when the ANOVA test was significant, differences between time points were investigated using Tuckey HSD post-hoc test. For community analysis (including alpha and beta diversity analyses) we have used the vegan package [45]. To find OTUs that are significantly different between multiple conditions (Degradation), DESeqDataSetFromMatrix() function from DESeq2 [46] package with the adjusted p-value significance cut-off of 0.05 and log2 fold change cut-off of 2 was used. Vegan's adonis() was used for analysis of variance (henceforth referred to as PERMANOVA) using distance matrices (BrayCurtis/Unweighted Unifrac/Weighted Unifrac for gene sequences) i.e., partitioning distance matrices among sources of variation

(Degradation). The scripts for above analysis can be found at http://userweb.eng.gla.ac.uk/umer.ijaz/#bioinformatics

Results

Design and optimization of *glnA* primers

Three new forward *glnA* primers (GSFw1200, GSFw900 and GSFw800) were designed to target a conserved region in groups 3, 4, 5, 7 and 8 of the *glnA* alignment (Additional file 4: Figure S1) at a position ≈120 bp, ≈380bp and ≈500bp, respectively, in front (closer to the 5' end of the gene) of an updated reverse primer from Hurt and co-workers named, GS1_new primer. This resulted in three amplicon sizes to derive a ratio amplicon (R_{amp}) from (Fig. 1). The newly designed primers (Table 1) were optimised for PCR and RT-PCR resulting in amplicons of the expected size for all primer pairs. Assays were subsequently optimised for SYBR Green Q-PCR. All primers except for GSFw800, producing the 500 bp amplicon were successfully optimised with diagnostic single peak melt curves. As such we proceeded with two R_{amp} ratio primer sets the R_{amp} 380/120 and the R_{amp} 380/170.

Heat degradation

Incubation of RNA at 90°C had a strong and rapid impact on its integrity with a drop in the RIN from 7.5 to 4.7 after 10min. At this point, the band corresponding to 23S rRNA had almost completely disappeared. Further exposure resulted in more pronounced degradation with accumulation of short RNA fragments and a RIN around 2 for both 45min and 90min exposure (Fig. 2A & 1A). One-way ANOVA revealed significant difference between all time-points, except 45 and 90min. A low and non-significant decrease in both R_{amp} indexes was observed (-0.07 for 380/120 and -0.11 for 380/170) between 0min and 10min (Fig. 2C). This would tend to indicate that the R_{amp} was less sensitive than the RIN for monitoring RNA

397 degradation by heat. However, interestingly the increase in Ct was also not significant for
398 both *amoA* and *16S rRNA* between 0 and 10min (Fig. 2B), showing that the R_{amp} reflected the
399 outcome of the RT-Q-PCR assays better than the RIN. Further exposure to heat induced a
400 more pronounced decrease in both R_{amp} (≈ -0.4 for 380/120 and ≈ -0.3 for 380/170) at 45min
401 compared to 0min. Both R_{amp} indexes reached values around 0.15 at 90min, which mapped
402 well the behaviour of *amoA*, with a sharp increase in the Ct for this transcript between 10 and
403 45min (≈4cts) and between 45 and 90min (another ≈4cts). The 16S rRNA transcript was also
404 affected but to a smaller extent (increase in Ct of only ≈3ct between 0 and 90min). Yet, in this
405 case too, the increase was quite low between 0 and 10min and sharper between 10-45min and
406 45-90min.
407
408 **UV degradation**
409 The RIN was almost insensitive to UV radiation with an overall decrease of ≈1 at 90min
410 compared to 0min (Fig. 3A & 3C). In contrast, UV radiation had a more pronounced effect
411 on transcript quantification than heat as reflected by a quasi linear increase in Ct of the *amoA*
412 transcript between 0 and 45min (Fig. 3B). Unlike heat exposure, 10min under UV induced
413 strong and significant increase in *amoA* Ct values (≈4cts). At 45min, the Ct had increased by
414 ≈9 compared to the starting point. After 90min, the Ct of the *amoA* transcript almost reached
415 35, close to the detection limit. The Ct for *16S rRNA* transcript increased steadily from 18 at
416 0min to 20 at 90min, showing that this assay/transcript was less sensitive to UV degradation.
417 The behaviour of the R_{amp}, again, mapped well onto *amoA* behaviour with a decrease of ≈0.2
418 after 10min exposure for both indexes (though this was not significant) (Fig. 3C). A net
419 decrease was observed at 45min (≈ -0.6 compared to 0min) and at 90min both R_{amp} almost
420 reached 0 since the Ct of the amplicon 3 *glnA* (380bp) was very close to 35.
421

Degradation by RNaseI

The RIN showed a rapid response to RNase I degradation with a decrease from 7.1 to 6 between 0 and 2U/µg (Fig. 4A & 4B.) as seen on virtual gels and electropherograms with an almost complete disappearance of the 23S rRNA. When using 10U/µg and higher concentrations, the RIN decreased and remained stable at approximately 2.5 indicating advanced/almost complete degradation of the RNA. Complete destruction of both rRNA and an accumulation of small size RNA molecules on the electropherogram can be observed (Fig 4A). In contrast, enzymatic degradation by RNase I had a relatively small effect on the Ct of the *amoA* transcript at low concentration (only 0.2 Ct increase between 0U/µg and 2U/µg treatments) (Fig. 4B). Ct values for *amoA* increased with greater degradation of the parent RNA (3 Cts difference at 10 and 20U/µg and 5 Cts at 40U/µg compared to 0U/µg control). Of note, *amoA* transcripts were still quantified from the degraded 40U/µg treatment with a mean Ct of 31.8. RNase I seemed to be the most effective treatment for the destruction of rRNA. Indeed, an increase of ≈ 3.2 Cts for the *16S rRNA* transcript was observed between 0 and 40U/µg treatments whereas an increase of only 2.2 Cts was observed between 0 and 90min for both physical degradation techniques (heat and UV). R_{amp} indexes were only slightly affected by 2U RNAseI/µg (decrease of ≈0.015 for 380/120 and ≈0.03 for 380/170) (Fig. 4C.). The decrease was more pronounced for both R_{amp} at higher concentrations of RNaseI (≈0.25 decrease at 20U/µg compared to 0U control). Even at concentrations as high as 40U/µg the R_{amp} indexes only reached 0.3. This indicated that at the high nuclease concentrations, even the small amplicons (120 and 170bp) were starting to degrade. In this experiment, the R_{amp} 380/170 seemed to be more sensitive than the R_{amp} 380/120 in mapping RNA degradation, with significant differences between 0 and 10U/µg treatments whereas R_{amp} 380/120 values only became significantly different from 0U control from 20U/µg. Again, as observed in the other degradation experiments, the behaviour of the *amoA* Ct was

447 better reflected by changes in R_{amp}, especially R_{amp} 380/170, rather than by changes in the
448 RIN.
449
450 **Effect of freeze/thaw cycles**
451 The effect of repeated cycles of freeze thaw on RNA is still poorly understood (and rarely
452 studied) as conflicting results are reported, yet this is a common cause for concern when
453 working with RNA. In our experiments, repeated freeze/thaw cycle (up to 10) did not induce
454 any noticeable effects on RNA integrity, whether monitored via RIN or R_{amp} (data not shown).
455 The effect of long term storage was also investigated but no effect could be seen after four
456 months storage at -80°C.
457
458 **Comparison between R_{amp} and RIN**
459 Data generated from all of the degradation experiments undertaken (UV, heat and RNaseI)
460 was compiled to determine which of the two integrity indexes (RIN VS R_{amp}) reflected the
461 degradation status of the *amoA* and 16S rRNA transcripts more closely as determined by RT-
462 Q-PCR. This was done by calculating Kendall correlations between either the R_{amp} or the RIN
463 and the Cts of the two gene transcript targets (Fig 5). When considering all three degradation
464 experiments, that is UV, heat and *RNaseI*, the RIN was not significantly correlated with 16S
465 rRNA nor *amoA* Ct values (p.value > 0.05). In contrast, the R_{amp} 380/170 ratio resulted in a
466 significant correlation with both *amoA* and 16S rRNA transcripts. The shorter R_{amp} 380/120
467 ratio was significantly correlated with *amoA* only (Fig 5A). However, as the RIN was almost
468 insensitive to UV, with a decrease of only about ≈1 after 90min exposure (Fig. 2), Kendall
469 correlations were repeated without the inclusion of the UV data set. In this case, both the RIN
470 and the R_{amp} were significantly correlated with 16S rRNA and *amoA* transcript abundances
471 within the degraded RNA samples (Fig. 5B). In fact, the RIN was better correlated with

amoA than 16S rRNA Cts. Nevertheless, both R_{amp} ratios were more highly correlated with *amoA* Cts than the RIN. Furthermore, the R_{amp} approach was more highly correlated with the 16S rRNA than the RIN. Taken together, these two observations confirm that the R_{amp} indexes better reflected RT-Q-PCR changes induced by RNA degradation than the RIN.

Effect of RNA degradation on transcript community composition

RNA degradation impacted upon *amoA, glnA* and *16S rRNA* gene quantification, as demonstrated previously. However, whether all members of the community were affected equally was still to be determined. To answer this question, cDNA amplicons of the Bacterial 16S rRNA, *amoA* and *glnA* transcripts underwent Illumina MISeq amplicon sequencing from all degradation points of the RNase I experiment representing RNA with RIN values from 7.5 to 2.4 and R_{amp} values from ≈0.8 to ≈0.3 and from ≈0.7 to ≈0.3 for Ramp 380/170 and Ramp 380/120 respectively. The effect of RNaseI treatment on community evenness was tested using PERMANOVA. Results are presented in Table 2 and figures 6, 7 and 8. Interestingly, the community structure of the three transcripts studied responded differently.

Strikingly, RNase I treatment had little effect on *16S rRNA* transcript community evenness (Fig 6A). Indeed, for individual OTUs, none of the members of the community were significantly differentially represented (*p*.value $\log_2$ difference >0.05) within highly degraded samples in comparison to controls (Fig 6B). For individual OTU's at least 90% had their relative expression change over the degradation experiment fall within the [-log2(1.5); lod2(1.5)] interval, even when comparing controls to the completely degraded 40U RNase I sample (Fig 6B). This indicates that *16S rRNA* OTU transcript community was responding evenly to degradation, with each member having the same chance to be affected regardless of its abundance or sequence.

For bacterial *amoA* transcript community there was no change in the overall composition with increasing degradation as reflected by the non-significant PERMANOVA (p.value >0.05). However, with increasing degradation, there was an increasing difference in the community evenness among replicates. Furthermore, unlike 16S rRNA transcripts, when examining individual *amoA* OTUs it was evident that in the degraded samples some OTUs were differentially represented at a significant level compared to controls (Fig. 7B). In fact, some OTUs in the highly degraded samples (10, 20 and 40U RNase I) had a fold change difference of up to 2 orders of magnitude compared to the controls and in most cases, resulting in their over representation in degraded samples (see Additional file 3). Moreover, in the more highly degraded treatments (10, 20 and 40U RNase I), up to 44% of *amoA* OTUs had their relative expression outside the [-log2(1.5); log2(1.5)] interval, compared to the starting RNA (Fig 7 B). So while there was not an overall significant difference in *amoA* community structure with increasing RNA degradation, there were changes in the relative expression of individual OTUs. The lack of overall statistical significance in community structure may in fact be explained by the overall lower numbers of *amoA* OTUs for comparison and the increasing difference among replicates in the degraded samples.

The effect of RNase I treatment was much more pronounced for *glnA* transcripts, than for *amoA,* and a significant change in community composition with increasing degradation was observed (p.value< 0.05 for PERMANOVA with both Bray-Curtis and Unifrac distances) (Fig 8A & 8B). As seen with *amoA*, the difference in community composition between replicates also increased with increasing RNase I treatment. Moreover, this effect was also observed at individual OTU level with a large fraction of the individual OTUs showing different expression levels in treated samples compared to controls (Fig. 8B). As seen for *amoA*, some *glnA* OTUs were highly over represented in degraded samples by 2 to 3 orders of magnitudes (Additional file 3), *e.g.* when comparing the untreated samples (NT) to the

521 40URNase samples, 0.28% (3 sequences) were over represented by 2 orders of magnitude.
522 When comparing the samples treated with buffer only to the 40URNase samples, 2.43% (19
523 sequences) were over represented by 2 orders of magnitude and 0.13% (1 sequence) by 3
524 orders of magnitude.
525
526 **Discussion**

527 Here we successfully designed and tested the Ratio Amplicon, $R_{amp,}$ index. The
528 concept is that as RNA degrades, longer strands are preferentially affected and the abundance
529 of the longer amplicon relative to the shorter amplicon will decrease with increasing RNA
530 degradation [18]. Using experimentally degraded environmental RNA we have shown that the
531 newly developed R_{amp} index was a better predictor of the Ct of the target mRNA transcript
532 used in this study, *amoA,* than the ribosome based RIN approach. In fact, when data from the
533 three degradation experiments carried out was considered together only the R_{amp} statistically
534 correlated with *amoA* Cts. As the RIN failed to detect UV degradation, we removed this data
535 from the correlations calculation to determine if this data set was biasing the results towards
536 the R_{amp} approach. In this case, there was also a significant correlation between the RIN and
537 *amoA* Ct (-0.51). However, the R_{amp} index still reflected the fate of the mRNA better than the
538 RIN (-0.72 and -0.77 for R_{amp} 380/120 and R_{amp} 380/170 respectively).

539 Taking the different RNA degradation approaches used individually, the RIN and R_{amp}
540 ratios responded differently. As noted above, the RIN did not change over a 90-minute
541 exposure to UV. UV causes intramolecular crosslinking of thymines but does not cause strand
542 breaks [47] while the RIN monitors stand break. Similar results were obtained by Bjorkman *et*
543 *al* [18] who reported a lack of response for the RIN and the RQI when human RNA
544 preparations were degraded by UV radiation, even after 120 minutes of exposure. As such
545 RNA damage by UV can't be detected by electrophoresis separation but is recorded by RT-Q-

546 PCR R_{amp} index. Other RNA degradation processes that result in base destruction but not
547 necessarily strand break include oxidative damage [48] or chemically-induced radical
548 formation [49].

549 In contrast, the RIN was the most efficient method to detect heat degradation. There
550 was a strong and significant decrease in this index after 10 minutes whereas the R_{amp} indexes
551 only became significantly different from the controls after 45 minutes. Moreover, there was
552 very little effect on the direct quantification of the transcripts by RT-Q-PCR with very little
553 change in the Ct of either *amoA* or 16S rRNA in the first 10 minutes at 90°C. Initially, heat
554 degradation caused a rapid decrease in the RIN. However, at this point the RT-Q-PCR targets
555 were actually responding more slowly and were more closely mapped by the R_{amp} than the
556 RIN. Björkman *et al* [18] showed a similar response of their differential amplicon, the
557 ΔΔamp index, that didn't change much between 2 and 10 min at 95°C whereas the RIN
558 rapidly reduced from 7 to 2. Moreover, Gingrich *et al* [50] showed that transcripts could be
559 quantified from RNA preparations incubated at 90°C for several hours. This relatively low
560 impact of heat on RNA quantification may be due to modification of RNA secondary
561 structures which could result in more efficient cDNA synthesis and mask the effect of the
562 heat-induced reduction of RNA integrity. More likely it is due to the small amplicon size of
563 the targets that are unaffected by degradation. This essentially illustrates the difference in the
564 methods used to monitor RNA degradation - the RIN detects strand break no matter where the
565 fracture occurs along the transcript while the R_{amp}, will only detect degradation if the break
566 occurs between primer binding sites.

567 RNA degradation using the nuclease enzyme RNase I was monitored using both RIN
568 and R_{amp}. A similar behaviour could be observed here as in the heat degradation experiment
569 with the RIN responding more quickly but loosing sensitivity when RNA was highly
570 degraded whereas the R_{amp} responded slightly later but remained sensitive when RNA was

571 extensively degraded. RNase I was the degradation method that had the strongest effect on the
572 16S rRNA Ct. RNase I activity is dependent on the concentration of the substrate. If rRNA
573 and mRNA are considered as two distinct substrates, it can be expected that RNase I will have
574 a greater impact on ribosomes as they constitute 80-85% of total RNA. Furthermore, cDNA
575 synthesis from mRNA would be enhanced in preparations where rRNA was depleted [51].
576 This dynamic may mask and change the effect of degradation over time, which would explain
577 the relatively low increase in Ct for *amoA* at the beginning of the RNase I degradation
578 experiment. Nevertheless, in this experiment and generally, for all degradation tests carried
579 out, the behaviour of the *amoA* Ct was better predicted by the R_{amp}, as reflected by the higher
580 correlation coefficient between R_{amp} indexes and *amoA* Ct than the RIN (Fig. 5). As the *in-*
581 *vitro* half-life of different transcripts is not well understood and has been shown to vary [52–
582 54] further work is required to test the correlation of the R_{amp} against a larger range of
583 mRNAs. For ribosomal RNA, while the correlation between the R_{amp} index and 16S rRNA Ct
584 was lower than for *amoA,* it still correlated better with RNA degradation than the RIN. This
585 indicates that the outcome of 16S rRNA analysis was less affected by degradation than our
586 mRNA targets. There are two factors that may contribute to this, the reported greater
587 robustness of ribosomal RNA than mRNA and the shorter (~103 bp) 16S rRNA amplicon.
588 That ribosomal RNAs behave the same as mRNA has never been proven. On the contrary,
589 Sidova *et al* [55] showed that when natural *post-mortem* degradation occurs, rRNA is more
590 stable than mRNA. In this case, rRNA is a poor predictor of degradation of the mRNA
591 fraction, as supported by this work. As mRNA is subjected to more rapid decay to adjust to
592 the needs of the cell whereas rRNA are degraded only under certain stress conditions or when
593 defective [56] then these intrinsic differences in stability properties may also affect
594 degradation rates of the different class of RNA post-extraction. Therefore, based on this work
595 we can conclude that the R_{amp} was a better predictor of mRNA integrity than the RIN.

However, as we and others [18] have shown RNA responds differently to different types of degradation e.g. strand break verses intramolecular crosslinking of thymines, and as the exact and likely multiple causes of post-extraction degradation are unknown, we recommend that the RIN is used in conjunction with the R_{amp} to monitor RNA integrity.

Which R_{amp} to use?

Since, in practice, only one R_{amp} index is necessary, we recommend using the R_{amp} 380/170. In theory, the higher the difference between the two amplicons the more sensitive the index would be. We initially designed a 500bp *glnA* PCR amplicon however, the Q-PCR assay failed to produce a single diagnostic melt curve analysis. The R_{amp} 380/170 always had a higher value than the R_{amp} 380/120 which would indicate that the number of 170bp targets is higher than the 120bp. Since both are amplified from the same target, this is not possible and the explanation for this observation is the lower efficiency of the 120bp Q-PCR compared to the 170bp assay. In spite of this, both R_{amp} correlated similarly well overall with each degradation experiment, with R_{amp} 380/170 slightly more sensitive in the RNase I experiment.

Impact of experimental degradation of environmental RNA on ribosomal (16S rRNA) and mRNA (*amoA*) community diversity.

For complex environmental communities, the integrity of RNA is not only important to evaluate quantitative gene expression, but is also of significance if it adversely affects the relative abundance of transcript diversity. To examine this, we assessed changes in the community structure of the 16S rRNA, *amoA* and *glnA* transcripts from all fractions of the RNase I sequentially degraded RNA.

619 The results were surprising with successful amplicon sequencing even from highly degraded
620 samples. Nevertheless, the data did suggest a different response of 16S rRNA and mRNA
621 transcripts to degradation, with 16S rRNA community structure unaffected over the range of
622 degraded RNA samples. That is a statistically similar community was present in the control
623 non-degraded samples as in the totally destroyed 40 Units RNase I (with a mean RIN of 2.5
624 and R_{amp} of 0.32 and 0.27 for R_{amp} 380/120 and Ramp 38/170 respectively). This indicates that
625 while total RNA was degraded, the small transcript fragments required for RT-PCR and
626 amplicon sequencing remained intact. In fact, so much so that no significant change in the
627 relative abundance of individual OTUs was observed.

628 On the other hand, RNA degradation had a greater influence on both *amoA* and *glnA* mRNA
629 targets. While, again surprisingly, transcript amplicons were successfully detected from all
630 degradation status samples, greater variability between degraded replicates was observed.
631 This resulted in statistically different communities for *glnA* but not *amoA* when compared to
632 the same non-degraded control samples. However, the low number of *amoA* OTUs and
633 increased variability between replicates contributed to the lower statistical power resulting in
634 no statistical difference between treatments (Fig. 6). Furthermore, there were significant,
635 sometimes up to 2 to 3 orders of magnitude change in the relative abundance of individual
636 *glnA* and *amoA* OTUs in the degraded samples verses control samples. So, while we could
637 successfully amplify mRNA transcripts from degraded environmental samples, we have
638 shown that the relative composition of the community members was adversely affected by
639 degradation and was not representative of the initial starting point. While further work is
640 needed to determine the impact of degradation across the entire transcriptome to see if all
641 mRNA's respond in a similar manner, it is clear from our mRNA amplicon sequencing that
642 RNA degradation will alter the outcome of community analysis. It is therefore necessary to
643 ensure the RNA integrity of the sample is known prior to interpretation of results. For this our

644 data indicates that a combination approach targeting both ribosomal (the RIN) and mRNA
645 (the R_{amp}) is needed.

646

647 **Best Practice for Environmental RNA**

648 The challenge when working with environmental samples will always be to retrieve RNA of a
649 high enough quality and integrity. Here we started with RNA extracted from marine
650 sediments that had an average RIN of ≈7 and R_{amp} of ≈0.8. This is the best quality RNA we
651 could produce with this beat-beating co-extraction method [36] and it already falls at the
652 lower end of acceptable RIN for pure culture [10]. Therefore, methods to improve the initial
653 quality of RNA extractions should also be a high priority, although this will be easier in some
654 environments than others. Improvement of extraction methods is crucial as it can lead to
655 important differences in the results. For example Feike *et al* [57] showed that different
656 sampling techniques influenced the relative abundance of transcripts retrieved from the
657 suboxic zone of the Baltic Sea. Next, the integrity of the extracted RNA should be
658 determined, and it should be ensured that the integrity value is similar among samples to be
659 compared. Here the R_{amp} approach should be a useful tool to complement current
660 electrophoretic approaches, such as the RIN prior to extensive downstream analysis.

661 Another consideration raised by this work is in the very fact that the differential amplicon
662 approach works. This shows that small cDNA amplicons can still be produced from highly
663 degraded RNA samples whereas long amplicons tend to disappear quickly. When using RNA
664 samples of poor quality, the comparison of expression levels between different targets might
665 be irrelevant if the difference in length of the RT-Q-PCR targets between genes is large. In
666 this case it would be better to use only small amplicons, that are less sensitive to degradation
667 [58]. An alternative, to deal with samples with different degradation status, potentially could

668 be to normalize RT-Q-PCR data to RNA integrity. A RIN based algorithm has been proposed
669 by Ho-Pun-Cheung *et al* [59] to reduce RT-Q-PCR errors due to RNA degradation in cancer
670 biopsies. In our case however, R_{amp} indexes correlated better than the RIN with *amoA* and 16S
671 rRNA Cts, making them better potential candidates as normalisation metrics. Therefore we
672 tested a normalisation coefficient based on the R_{amp} (Additional file 2; Figure S2). As in Ho-
673 Pun-Cheung *et al* [59], we assumed a linear relationship between the integrity index and the
674 changes in transcript Cts (*i.e.* change in Ct = α x change in R_{amp}). This assumption facilitated
675 the calculation of a regression coefficient α that was used to normalize Cts as explained in
676 figure S2. Although the use of such normalization reduced the errors attributable to RNA
677 degradation (Additional file 2; Figure S2.), several limitations remain: 1) the linear
678 relationship between changes in Cts and R_{amp} might not always be true depending on the
679 transcript tested, 2) the regression coefficient α depends on the degradation technique
680 (Additional file 2; Table S1), 3) the regression coefficient α depends on the transcript tested
681 (Additional file 2; Table S1) and 4) the regression coefficient α may depend on the
682 environment from which RNA was extracted. Until more work is done to validate such
683 normalization strategies, or to dramatically improve the quality of the RNA that can be
684 extracted from environmental samples [57], we recommend using integrity indexes
685 (differential amplicon and microfluidics based techniques) as initial quality checks of RNA
686 and advise not to make absolute comparisons among samples with dissimilar integrity status.

687

688 **Conclusion**

689 Assessing RNA quality is essential for obtaining meaningful transcriptomic results. The
690 current approach to monitor RNA integrity include the RIN and RQI. This is a useful
691 technique that is widely under-used (or reported) in microbial transcriptomics studies, to give

an overview of total RNA quality based on a ratio between the 23S and 16S ribosomes. Since most transcriptomics studies are interested in the metabolic function and therefore mRNA, it would be preferable to have an integrity index to target the mRNA. Furthermore, it is unknown if degradation of rRNA reflects mRNA degradation. We therefore developed and experimentally tested a new index, the R_{amp}, the goal of which was to specifically target mRNA degradation and we showed that it performed better than the RIN at predicting the outcome of RT-Q-PCR of a functional gene (*amoA*). It was shown in this study that both quantitative (RT-Q-PCR) and qualitative (sequencing) results can be obtained, even from very degraded samples. Comparison of gene expression level between preparations with different degradation levels can therefore lead to false conclusions if integrity is not checked prior to analysis. Thus, we encourage microbial ecologists to report integrity indexes in order to improve reproducibility and facilitate comparison between transcriptomics studies. For this we propose that a R_{amp} ratio is used alongside the RIN.

Abbreviations

R_{amp}: Ratio Amplicon; RIN: RNA Integrity number; RQI: RNA Quality Score; RT-(Q)-PCR: Reverse Transcriptase (Quantitative) Polymerase Chain Reaction; cDNA: complementary DNA; Ct: Cycle threshold

Ethics approval and consent to participate

Not applicable

Consent for publication

Not applicable

Competing interest

The authors declere that they have no competing interest

Authors' contribution

CJS supervised the project. CJS and FC designed the experiments. FC carried out the experiments. FC and CJS analysed the RT-Q-PCR and RIN measurment data. FC and UZI ran the bioinformatic pipeline for amplicon sequences processing. FC, CJS, UZI and analysed the amplicon sequencing results. FC, UZI, CJS and wrote the manuscript. All authors read and approved the final manuscript.

Data availability

Ct and RIN data presented in this study are provided in additionnal file 7. The sequencing data are available on the European Nucleotide Archive under the study accession number: PRJEB28215 (http://www.ebi.ac.uk/ena/data/view/PRJEB28215) with information about the samples given in additional file 5 and 6.

Acknowledgements

We would like to thank Dr. Aoife Duff for collecting the sediment samples.

Funding

FC was supported by a Univeristy of Glasgow, School of Engineering EPSRC Doctoral Scholarship; UZI was funded by NERC IRF NE/L011956/1; CJS was supported by the Royal Academy of Engineering under the Research Chairs and Senior Research Fellowships scheme (RCSRF1718643).

742 **References**

743 1. Medini D, Serruto D, Parkhill J, Relman DA, Donati C, Moxon R, et al. Microbiology in
744 the post-genomic era. Nat Rev Microbiol. 2008;6:419–30.
745 2. Moran MA, Satinsky B, Gifford SM, Luo H, Rivers A, Chan LK, et al. Sizing up
746 metatranscriptomics. ISME J. 2013;7:237–43. doi:10.1038/ismej.2012.94.
747 3. Evans TG. Considerations for the use of transcriptomics in identifying the "genes that
748 matter" for environmental adaptation. J Exp Biol. 2015;218:1925–35.
749 doi:10.1242/jeb.114306.
750 4. Smith CJ, Nedwell DB, Dong LF, Osborn AM. Evaluation of quantitative polymerase
751 chain reaction-based approaches for determining gene copy and gene transcript numbers in
752 environmental samples. Environ Microbiol. 2006;8:804–15.
753 5. Laalami S, Zig L, Putzer H. Initiation of mRNA decay in bacteria. Cell Mol Life Sci.
754 2014;71:1799–828.
755 6. Die J V, Román B. RNA quality assessment: a view from plant qPCR studies. J Exp Bot.
756 2012;63:6069–77.
757 7. Copois V, Bibeau F, Bascoul-Mollevi C, Salvetat N, Chalbos P, Bareil C, et al. Impact of
758 RNA degradation on gene expression profiles: Assessment of different methods to reliably
759 determine RNA quality. J Biotechnol. 2007;127:549–59.
760 8. Fleige S, Pfaffl MW. RNA integrity and the effect on the real-time qRT-PCR performance.
761 Mol Aspects Med. 2006;27:126–39.
762 9. Fleige S, Walf V, Huch S, Prgomet C, Sehm J, Pfaffl MW. Comparison of relative mRNA
763 quantification models and the impact of RNA integrity in quantitative real-time RT-PCR.
764 Biotechnol Lett. 2006;28:1601–13.
765 10. Jahn CE, Charkowski AO, Willis DK. Evaluation of isolation methods and RNA integrity
766 for bacterial RNA quantitation. J Microbiol Methods. 2008;75:318–24.

767 11. Kaczanowska M, Ryden-Aulin M. Ribosome Biogenesis and the Translation Process in
768 Escherichia coli. Microbiol Mol Biol Rev. 2007;71:477–94. doi:10.1128/MMBR.00013-07.
769 12. Rhodes ME, Oren A, House CH. Dynamics and persistence of dead sea microbial
770 populations as shown by high-throughput sequencing of rRNA. Appl Environ Microbiol.
771 2012;78:2489–92.
772 13. McKillip JL, Jaykus L, Drake M. rRNA Stability in Heat-Killed and UV-Irradiated
773 Enterotoxigenic Staphylococcus aureus and Escherichia coli O157 : H7 rRNA Stability in
774 Heat-Killed and UV-Irradiated Enterotoxigenic Staphylococcus aureus and Escherichia coli
775 O157 : H7. Appl Environ Microbiol. 1998;64:4264–8.
776 14. Rathnayaka USK, Rakshit SK. The stability of rrna in heat-killed Salmonella enterica
777 cells and its detection by fluorescent in situ hybridisation (FISH). Trop Life Sci Res.
778 2010;21:47–53.
779 15. Hurt RA, Qiu X, Wu L, Roh Y, Palumbo A V, Tiedje JM, et al. Simultaneous Recovery of
780 RNA and DNA from Soils and Sediments. Appl Environ Microbiol. 2001;67:4495–503.
781 16. Die J V., Obrero Á, González-Verdejo CI, Román B. Characterization of the 3':5' ratio
782 for reliable determination of RNA quality. Anal Biochem. 2011;419:336–8.
783 doi:10.1016/j.ab.2011.08.012.
784 17. Dreyfus M, Régnier P. The poly(A) tail of mRNAs: Bodyguard in eukaryotes, scavenger
785 in bacteria. Cell. 2002;111:611–3.
786 18. Björkman J, Švec D, Lott E, Kubista M, Sjöback R. Differential amplicons (δAmp)-a new
787 molecular method to assess RNA integrity. Biomol Detect Quantif. 2016;6:4–12.
788 19. Karlsson O, Segerström L, Sjöback R, Nylander I, Borén M. qPCR based mRNA quality
789 score show intact mRNA after heat stabilization. Biomol Detect Quantif. 2016;7:21–6.
790 doi:10.1016/j.bdq.2016.01.002.
791 20. Reck M, Tomasch J, Deng Z, Jarek M, Husemann P, Wagner-Döbler I. Stool

792 metatranscriptomics: A technical guideline for mRNA stabilisation and isolation. BMC
793 Genomics. 2015;16:494. doi:10.1186/s12864-015-1694-y.
794 21. Kumada Y, Benson DR, Hillemann D, Hosted TJ, Rochefort D a, Thompson CJ, et al.
795 Evolution of the glutamine synthetase gene, one of the oldest existing and functioning genes.
796 Proc Natl Acad Sci U S A. 1993;90:3009–13.
797 22. Brown JR, Masuchi Y, Robb FT, Doolittlel WF. Evolutionary relationships of bacterial
798 and archaeal glutamine synthetase genes. J Mol Evol. 1994;38:566–76.
799 23. Reitzer L. Nitrogen Assimilation and Global Regulation in *Escherichia coli*. Annu Rev
800 Microbiol. 2003;57:155–76. doi:10.1146/annurev.micro.57.030502.090820.
801 24. Costa R, Gomes NCM, Milling A, Smalla K. An optimized protocol for simultaneous
802 extraction of DNA and RNA from soils. Brazilian J Microbiol. 2004;35:230–4.
803 25. Sharma S, Mehta R, Gupta R, Schloter M. Improved protocol for the extraction of
804 bacterial mRNA from soils. J Microbiol Methods. 2012;91:62–4.
805 doi:10.1016/j.mimet.2012.07.016.
806 26. Sessitsch A, Gyamfi S, Stralis-Pavese N, Weilharter A, Pfeifer U. RNA isolation from soil
807 for bacterial community and functional analysis: evaluation of different extraction and soil
808 conservation protocols. J Microbiol Methods. 2002;51:171–9. doi:S0167701202000659 [pii].
809 27. Atkinson MR, Blauwkamp T a, Bondarenko V, Studitsky V, Ninfa AJ. Activation of the
810 glnA, glnK, and nac Promoters as Escherichia coli Undergoes the Transition from Nitrogen
811 Excess Growth to Nitrogen Starvation. Society. 2002;184:5358–63.
812 28. Hua Q, Yang C, Oshima T, Mori H, Shimizu K. Analysis of Gene Expression in
813 Escherichia coli in Response to Changes of Growth-Limiting Nutrient in Chemostat Cultures.
814 Society. 2004;70:2354–66. doi:10.1128/AEM.70.4.2354.
815 29. Leigh JA, Dodsworth JA. Nitrogen Regulation in Bacteria and Archaea. Annu Rev
816 Microbiol. 2007;61:349–77. doi:10.1146/annurev.micro.61.080706.093409.

817 30. Duff AM, Zhang LM, Smith CJ. Small-scale variation of ammonia oxidisers within
818 intertidal sediments dominated by ammonia-oxidising bacteria Nitrosomonas sp. amoA genes
819 and transcripts. Sci Rep. 2017;7:1–13. doi:10.1038/s41598-017-13583-x.
820 31. Zhang L, Duff A, Smith C. Community and functional shifts in ammonia oxidizers across
821 terrestrial and marine (soil/sediment) boundaries in two coastal Bay ecosystems. Environ
822 Microbiol. 2018;00.
823 32. Clark K, Karsch-Mizrachi I, Lipman DJ, Ostell J, Sayers EW. GenBank. Nucleic Acids
824 Res. 2016;44:D67–72.
825 33. Altschul SF, Gish W, Miller W, Myers EW, Lipman DJ. Basic local alignment search
826 tool. J Mol Biol. 1990;215:403–10. doi:10.1016/S0022-2836(05)80360-2.
827 34. Edgar RC. MUSCLE: Multiple sequence alignment with high accuracy and high
828 throughput. Nucleic Acids Res. 2004;32:1792–7.
829 35. Kumar S, Stecher G, Tamura K. MEGA7: Molecular Evolutionary Genetics Analysis
830 Version 7.0 for Bigger Datasets. Mol Biol Evol. 2016;33:1870–4.
831 36. Griffiths RI, Whiteley AS, O'Donnell AG, Bailey MJ. Rapid method for
832 coextraction of DNA and RNA from natural environments for analysis of ribosomal DNA-
833 and rRNA-based microbial community composition. Appl Environ Microbiol. 2000;66:5488–
834 91.
835 37. Winter DJ. rentrez: An R package for the NCBI eUtils API. R J. 2017;9:520–6.
836 doi:10.7287/peerj.preprints.3179v2.
837 38. Joshi NA, Sickle JNF. A sliding-window, adaptive, quality-based trimming tool for FastQ
838 files. 2011;:1–9.
839 39. Nikolenko SI, Korobeynikov AI, Alekseyev MA. BayesHammer: Bayesian clustering for
840 error correction in single-cell sequencing. BMC Genomics. 2013;14 Suppl 1:1–11.
841 40. Schirmer M, Ijaz UZ, D'Amore R, Hall N, Sloan WT, Quince C. Insight into biases and

842 sequencing errors for amplicon sequencing with the Illumina MiSeq platform. Nucleic Acids
843 Res. 2015;43.
844 41. D'Amore R, Ijaz UZ, Schirmer M, Kenny JG, Gregory R, Darby AC, et al. A
845 comprehensive benchmarking study of protocols and sequencing platforms for 16S rRNA
846 community profiling. BMC Genomics. 2016;17. doi:10.1186/s12864-015-2194-9.
847 42. Caporaso JG, Kuczynski J, Stombaugh J, Bittinger K, Bushman FD, Costello EK, et al.
848 QIIME allows analysis of high-throughput community sequencing data. Nat Methods.
849 2010;7:335–6. doi:10.1038/nmeth.f.303.QIIME.
850 43. Katoh K, Asimenos G, Toh H. Multiple Alignment of DNA Sequences with MAFFT. In:
851 Bioinformatics for DNA Sequence Analysis, Methods in Molecular Biology. 2009. p. 39–64.
852 doi:10.1007/978-1-59745-251-9.
853 44. Price MN, Dehal PS, Arkin AP. FastTree 2 - Approximately maximum-likelihood trees
854 for large alignments. PLoS One. 2010;5.
855 45. Oksanen J, Kindt R, O'Hara RB. vegan: Community Ecology Package. Available from
856 http://cc.oulu.fi/~jarioksa/. 2005;3 January. http://cc.oulu.fi/~jarioksa/.
857 46. Love MI, Huber W, Anders S. Moderated estimation of fold change and dispersion for
858 RNA-seq data with DESeq2. Genome Biol. 2014;15:1–21.
859 47. Kladwang W, Hum J, Das R. Ultraviolet Shadowing of RNA Can Cause Significant
860 Chemical Damage in Seconds. Sci Rep. 2012;2:517. doi:10.1038/srep00517.
861 48. Rhee Y, Valentine MR, Termini J. Oxidative base damage in RNA detected by reverse
862 transcriptase. Nucleic Acids Res. 1995;23:3275–82.
863 49. Hawkins CL, Davies MJ. Hypochlorite-induced damage to DNA, RNA, and
864 polynucleotides: Formation of chloramines and nitrogen-centered radicals. Chem Res
865 Toxicol. 2002;15:83–92.
866 50. Gingrich J, Rubio T, Karlak C. Effect of RNA degradation on the data quality in

867 quantitative PCR and microarray experiments. Bio-Rad Bull. 2008;:1–6. http://www.gmo-
868 qpcr-analysis.info/gingrich-bulletin-5547A.pdf.
869 51. Petrova OE, Garcia-Alcalde F, Zampaloni C, Sauer K. Comparative evaluation of rRNA
870 depletion procedures for the improved analysis of bacterial biofilm and mixed pathogen
871 culture transcriptomes. Sci Rep. 2017;7 May 2016:41114. doi:10.1038/srep41114.
872 52. Belasco JG. All Things Must Pass: Constrasts and Commonalities in Eukaryotic and
873 Bacterial mRNA Decay. Nat Rev Mol Cell Biol. 2010;11:467–478.
874 53. Evguenieva-Hackenberg E, Klug G. New aspects of RNA processing in prokaryotes. Curr
875 Opin Microbiol. 2011;14:587–92. doi:10.1016/j.mib.2011.07.025.
876 54. Selinger WD, Saxena MR, Cheung K., Church MG, Rosenow C. Global RNA Half-Life
877 Analysis in. Genome Res. 2003; January:216–23.
878 55. Sidova M, Tomankova S, Abaffy P, Kubista M, Sindelka R. Effects of post-mortem and
879 physical degradation on RNA integrity and quality. Biomol Detect Quantif. 2015;5:3–9.
880 doi:10.1016/j.bdq.2015.08.002.
881 56. Deutscher MP. Degradation of RNA in bacteria: Comparison of mRNA and stable RNA.
882 Nucleic Acids Res. 2006;34:659–66.
883 57. Feike J, Jürgens K, Hollibaugh JT, Krüger S, Jost G, Labrenz M. Measuring unbiased
884 metatranscriptomics in suboxic waters of the central Baltic Sea using a new in situ fixation
885 system. ISME J. 2012;6:461–70.
886 58. Antonov J, Goldstein DR, Oberli A, Baltzer A, Pirotta M, Fleischmann A, et al. Reliable
887 gene expression measurements from degraded RNA by quantitative real-time PCR depend on
888 short amplicons and a proper normalization. Lab Invest. 2005;85:1040–50.
889 59. Ho-Pun-Cheung A, Bascoul-Mollevi C, Assenat E, Boissière-Michot F, Bibeau F, Cellier
890 D, et al. Reverse transcription-quantitative polymerase chain reaction: Description of a RIN-
891 based algorithm for accurate data normalization. BMC Mol Biol. 2009;10:1–10.

892 60. Hornek R, Pommerening-Röser A, Koops HP, Farnleitner AH, Kreuzinger N, Kirschner
893 A, et al. Primers containing universal bases reduce multiple amoA gene specific DGGE band
894 patterns when analysing the diversity of beta-ammonia oxidizers in the environment. J
895 Microbiol Methods. 2006;66:147–55.
896 61. Suzuki MT, Taylor LT, Delong EF, Long EFDE. Quantitative Analysis of Small-Subunit
897 rRNA Genes in Mixed Microbial Populations via 5′-Nuclease Assays Quantitative Analysis
898 of Small-Subunit rRNA Genes in Mixed Microbial Populations via 5 J -Nuclease Assays.
899 2000;66:4605–14.
900 62. Marchesi JR, Sato T, Weightman AJ, Martin TA, Fry JC, Hiom SJ, et al. Design and
901 evaluation of useful bacterium-specific PCR primers that amplify genes coding for bacterial
902 16S rRNA. Appl Environ Microbiol. 1998;64:795–9.
903 63. Lee TK, Van Doan T, Yoo K, Choi S, Kim C, Park J. Discovery of commonly existing
904 anode biofilm microbes in two different wastewater treatment MFCs using FLX Titanium
905 pyrosequencing. Appl Microbiol Biotechnol. 2010;87:2335–43.
906 64. Parada AE, Needham DM, Fuhrman JA. Every base matters: Assessing small subunit
907 rRNA primers for marine microbiomes with mock communities, time series and global field
908 samples. Environ Microbiol. 2016;18:1403–14.
909 65. Caporaso JG, Kuczynski J, Stombaugh J, Bittinger K, Bushman FD, Costello EK, et al.
910 correspondence QIIME allows analysis of high- throughput community sequencing data
911 Intensity normalization improves color calling in SOLiD sequencing. Nat Publ Gr.
912 2010;7:335–6. doi:10.1038/nmeth0510-335.

913

914 **Figure Legends**

915 **Fig 1. Schematic representation of primer binding sites along the Bacterial *glnA* gene.**
916 Primers are represented by arrows pointing to the right (forward primers) or to the left

(reverse primer). The amplicons (Amp) generated by the different primer combinations are represented as colored lines. The formulas used to calculate the two R_{amp} indexes are detailed under the figure.

Fig 2. Effect of heat degradation on RNA integrity measured via the RIN (A), with RT-Q-PCR (B) and RIN versus R_{amp} (C). For RIN, RNA integrity visualised in virtual gels (A; left) and electropherogram (A; right) are displayed against incubation period at 90°C. B) Effect of degradation on transcript quantification; Amp 1-3: average Ct (n=3) of one of the three possible *glnA* amplicons; *amoA*: average *amoA* Ct (n=3) of the Bacterial *amoA* transcript; *16S rRNA*: average *16S rRNA* Ct (n=3) of the bacterial *16S rRNA* transcript. Letters indicate the result of TukeyHSD tests (points with different letters had values significantly different from each other using 0.05 as threshold for the *p*.value). Effect of RNA degradation on R_{amp} index is presented in Fig. C. The R_{amp} 380/120 was calculated as $\frac{35-ct(Amp\ 3)}{35-ct(Amp\ 1)}$ and the Ramp 380/170 as $\frac{35-ct(Amp\ 3)}{35-ct(Amp\ 2)}$; For comparison, RIN values were also plotted.

Fig 3. Effect of UV degradation on RNA integrity measured via the RIN (A), with RT-Q-PCR (B) and RIN versus R_{amp} (C). For RIN, RNA integrity visualised in virtual gels (A; left) and electropherogram (A; right) are displayed against incubation period under UV. B) Effect of degradation on transcript quantification; Amp 1-3: average Ct (n=3) of one of the three possible *glnA* amplicons; *amoA*: average *amoA* Ct (n=3) of the Bacterial *amoA* transcript; *16S rRNA*: average *16S rRNA* Ct (n=3) of the bacterial *16S rRNA* transcript. Letters indicate the result of TukeyHSD tests (points with different letters had values significantly different from each other using 0.05 as threshold for the *p*.value). Effect of RNA degradation

on R_{amp} index is presented in Fig. C. The R_{amp} 380/120 was calculated as $\frac{35-ct(Amp\ 3)}{35-ct(Amp\ 1)}$ and the Ramp 380/170 as $\frac{35-ct(Amp\ 3)}{35-ct(Amp\ 2)}$; For comparison, RIN values were also plotted.

Fig 4. Effect of RNase I degradation on RNA integrity measured via the RIN (A), with RT-Q-PCR (B) and RIN versus R_{amp} (C). For RIN, RNA integrity visualised in virtual gels (A; left) and electropherogram (A; right) are displayed against incubation period with RNase I B) Effect of degradation on transcript quantification; Amp 1-3: average Ct (n=3) of one of the three possible *glnA* amplicons; *amoA*: average *amoA* Ct (n=3) of the Bacterial *amoA* transcript; *16S rRNA*: average *16S rRNA* Ct (n=3) of the bacterial *16S rRNA* transcript. Letters indicate the result of TukeyHSD tests (points with different letters had values significantly different from each other using 0.05 as threshold for the *p*.value). Effect of RNA degradation on R_{amp} index is presented in Fig. C. The R_{amp} 380/120 was calculated as $\frac{35-ct(Amp\ 3)}{35-ct(Amp\ 1)}$ and the Ramp 380/170 as $\frac{35-ct(Amp\ 3)}{35-ct(Amp\ 2)}$; For comparison, RIN values were also plotted.

Fig 5. Kendall correlations between integrity indexes and Cts of the two reference gene used in this study. The correlations coefficients were calculated using all data generated from UV, heat and RNaseI degradation experiments (left) and from the heat and RNase I only (right). Black crosses indicate absence of significant correlation (threshold: p value>0.05).

Fig 6. Effect of RNase I treatment on 16S rRNA transcript composition. Bar charts (A) represent changes in community composition of the 50 most abundant taxa. Scatterplots (B) represent log2 changes of individual taxa along the degradation gradient relative to control experiments (no treatment control (NT) or buffer only control (0URNaseI/µl)) as indicated by

963 black arrows. Taxa with a significant difference (*p*.value< 0.05) in expression greater than or
964 equal to a 2-fold change (positively or negatively) relative to controls are indicated in red.

965

966 **Fig. 7 Effect of RNase I treatment on *amoA* transcript composition.** Bar charts (A)
967 represent changes in community composition of the 50 most abundant taxa. Scatterplots (B)
968 represent log2 changes of individual taxa along the degradation gradient relative to control
969 experiments (no treatment control (NT) or buffer only control (0URNaseI/µl)) as indicated by
970 black arrows. Taxa with a significant difference (*p*.value< 0.05) in expression greater than or
971 equal to a 2-fold change (positively or negatively) relative to controls are indicated in red.

972

973 **Fig. 8 Effect of RNase I treatment on *glnA* transcript composition.** Bar charts (A)
974 represent changes in community composition of the 50 most abundant taxa. Scatterplots (B)
975 represent log2 changes of individual taxa along the degradation gradient relative to control
976 experiments (no treatment control (NT) or buffer only control (0URNaseI/µl)) as indicated by
977 black arrows. Taxa with a significant difference (*p*.value< 0.05) in expression greater than or
978 equal to a 2-fold change (positively or negatively) relative to controls are indicated in red.

979

980

981

982

983

984

985

986

Tables

Table 1 List of primers used in this study.

Primer	Sequence (5' → 3')	Orientation	Target	Experiment	Reference
GS1_new	GCTTGAGGATGCCGCCGATGTA	Reverse	Bacterial *glnA*, all amplicons	Q-PCR and sequencing	This study, modified from Hurt and co-workers (14)
GSFw1200	GGTTCGGGCATGCACGTGCA	Forward	Bacterial *glnA*, amplicon 1 (120bp)	Q-PCR	This study
GS2_new	AAGACCGCGACCTTNATGCC	Forward	Bacterial *glnA*, amplicon 2 (170bp)	Q-PCR	This study, modified from Hurt and co-workers (14)
GSFw900	GTCAARGGCGGYTAYTTCCC	Forward	Bacterial *glnA*, amplicon 3 (380bp)	Q-PCR and sequencing	This study
GSFw800	GAAGCCGAGTTCTTCSTCTTCGA	Forward	Bacterial *glnA*, amplicon 4 (540bp)	PCR	This study
BacamoA-1F BacamoA-2R	GGGGHTTYTACTGGTGGT CCCCTCBGSAAAVCCTTCTTC	Forward Reverse	Bacterial *amoA* gene (435bp)	Q-PCR and sequencing	[60]
1369F 1492R 1389P	CGGTGAATACGTTCYCGG GGWTACCTTGTTACGACTT CTTGTACACACCGCCCGTC	Forward Reverse Probe	Bacterial 16S rRNA gene (123 bp)	Q-PCR	[61]
F63 518R	CAGGCCTAACACATGGCAAGTC ATTACCGCGGCTGCTGG	Forward Reverse	Bacterial 16S rRNA V1→V3 (455bp)	PCR	[62] [63]

515F	GTG YCA GCM GCC GCG GTA A	Forward	Bacterial 16S rRNA	Sequencing	[64]
806R	GGA CTA CNV GGG TWT CTA AT	Reverse	V4 (291bp)		[65]

989

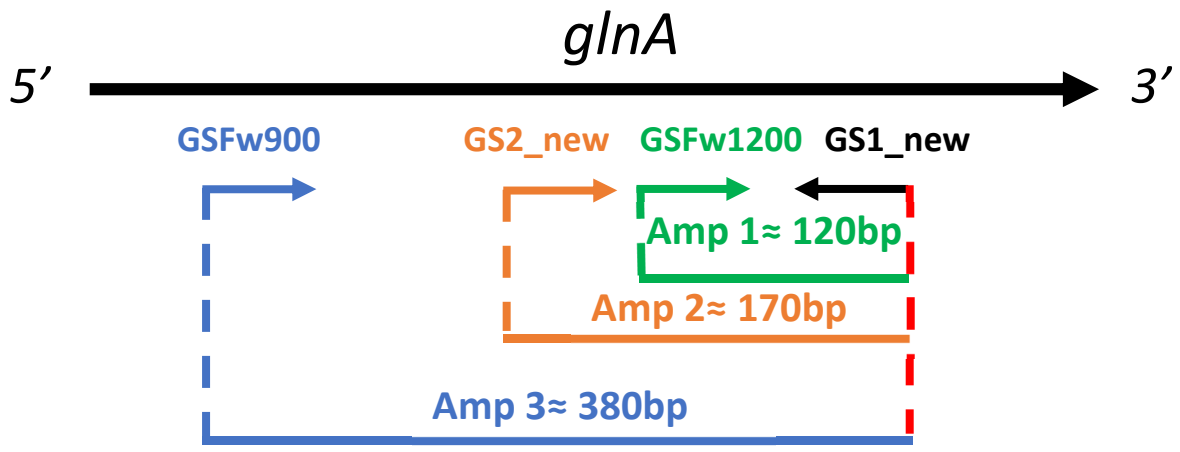

$$\textbf{Ramp 380/120} = \frac{\textbf{35−Ct Amp 3}}{\textbf{35−Ct Amp 1}}$$

$$\textbf{Ramp 380/170} = \frac{\textbf{35−Ct Amp 3}}{\textbf{35−Ct Amp 2}}$$

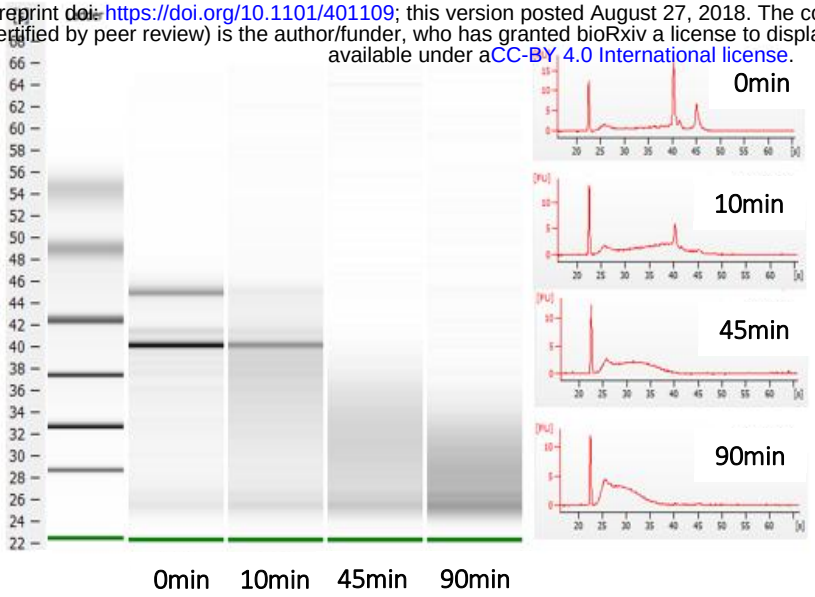

B

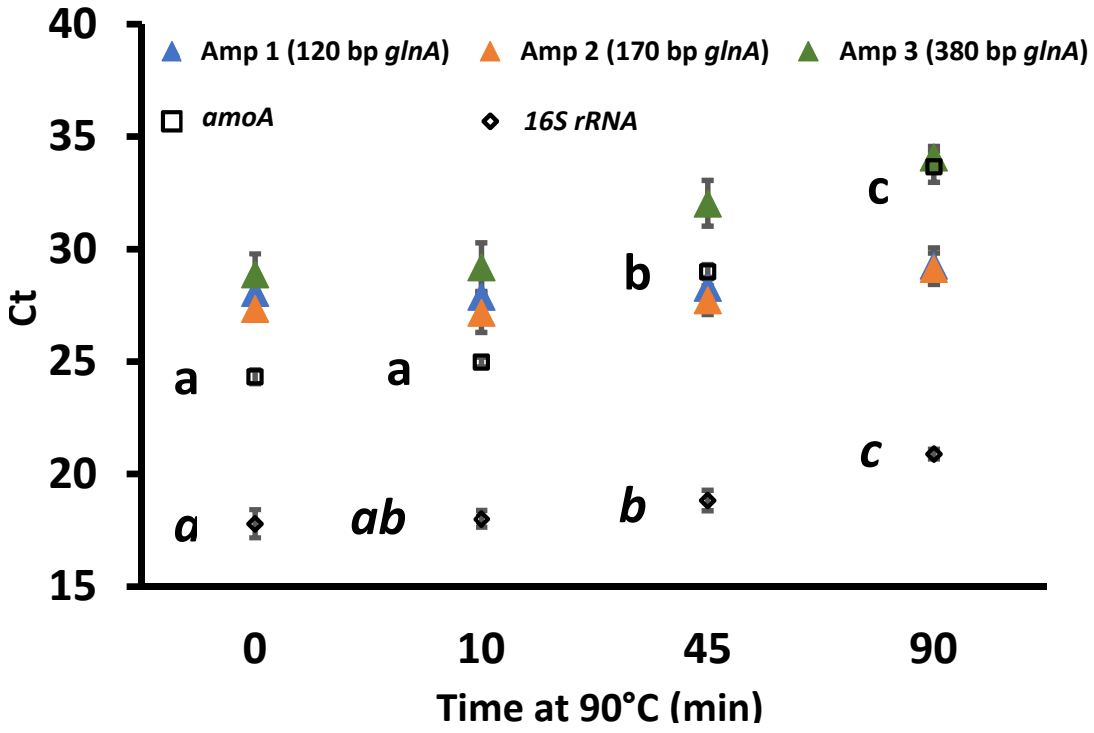

C

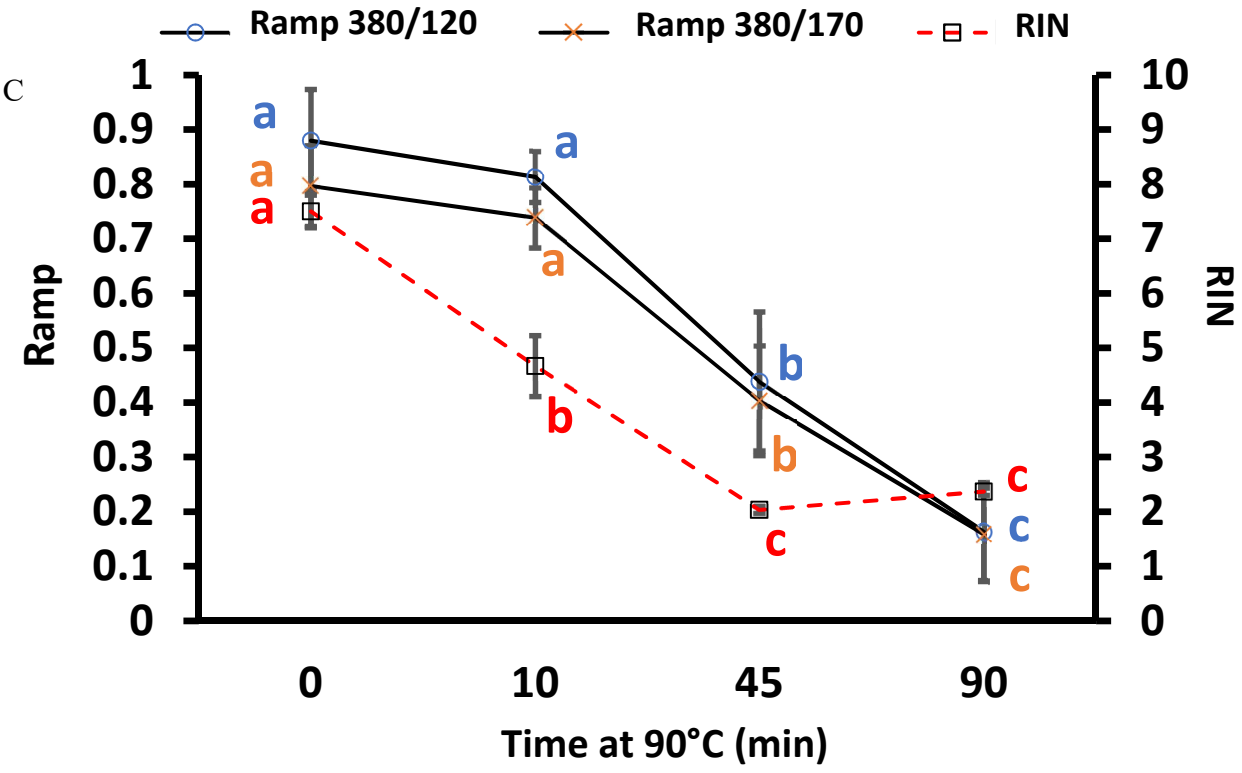

A

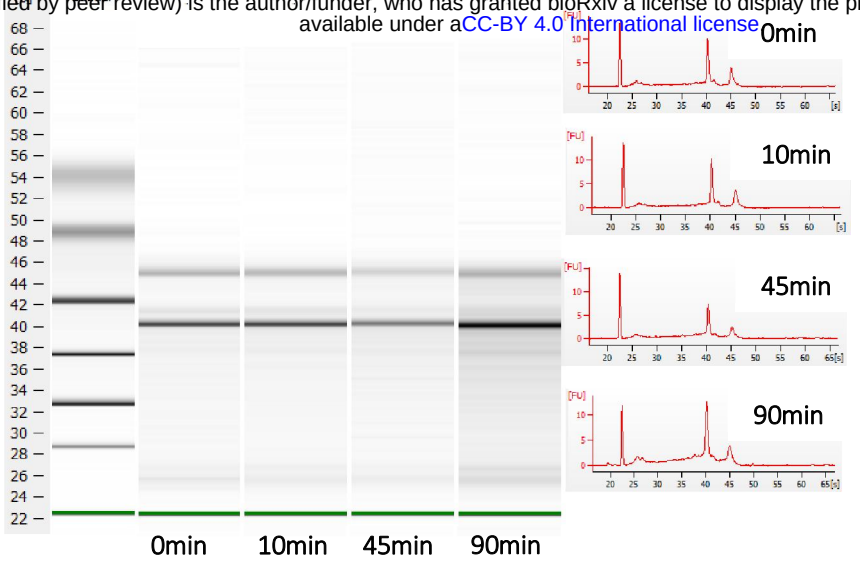

B

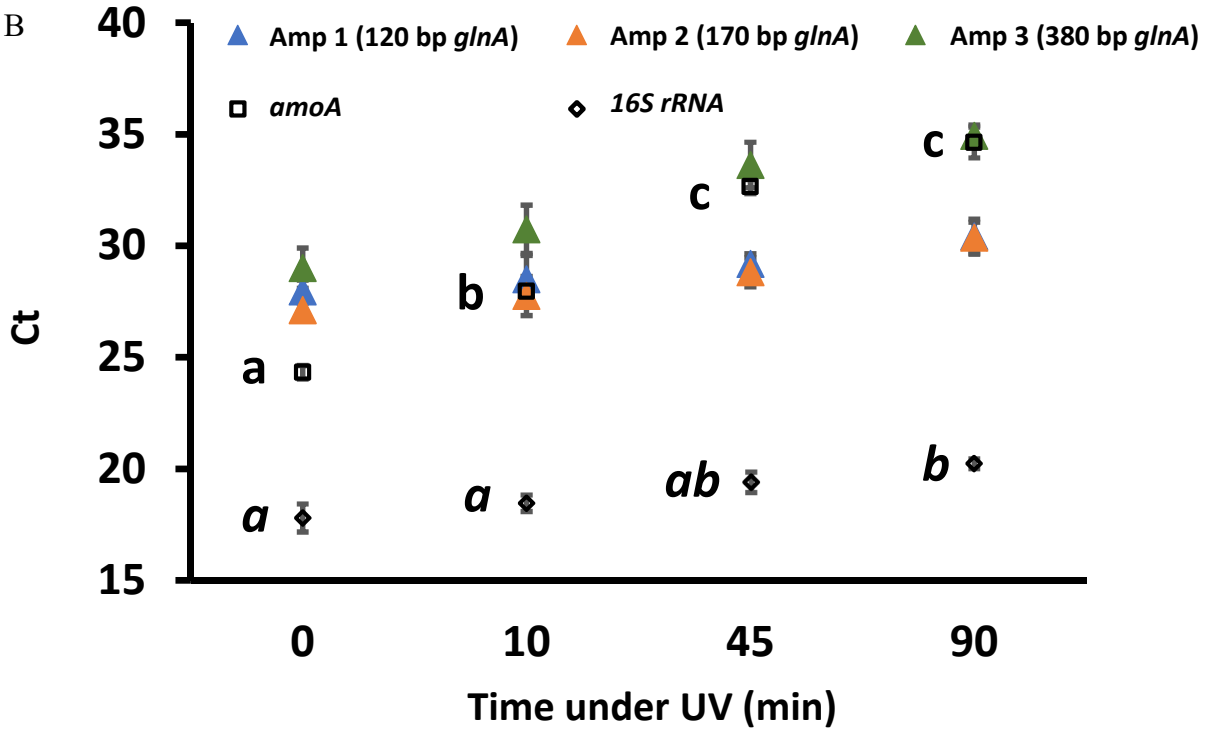

C

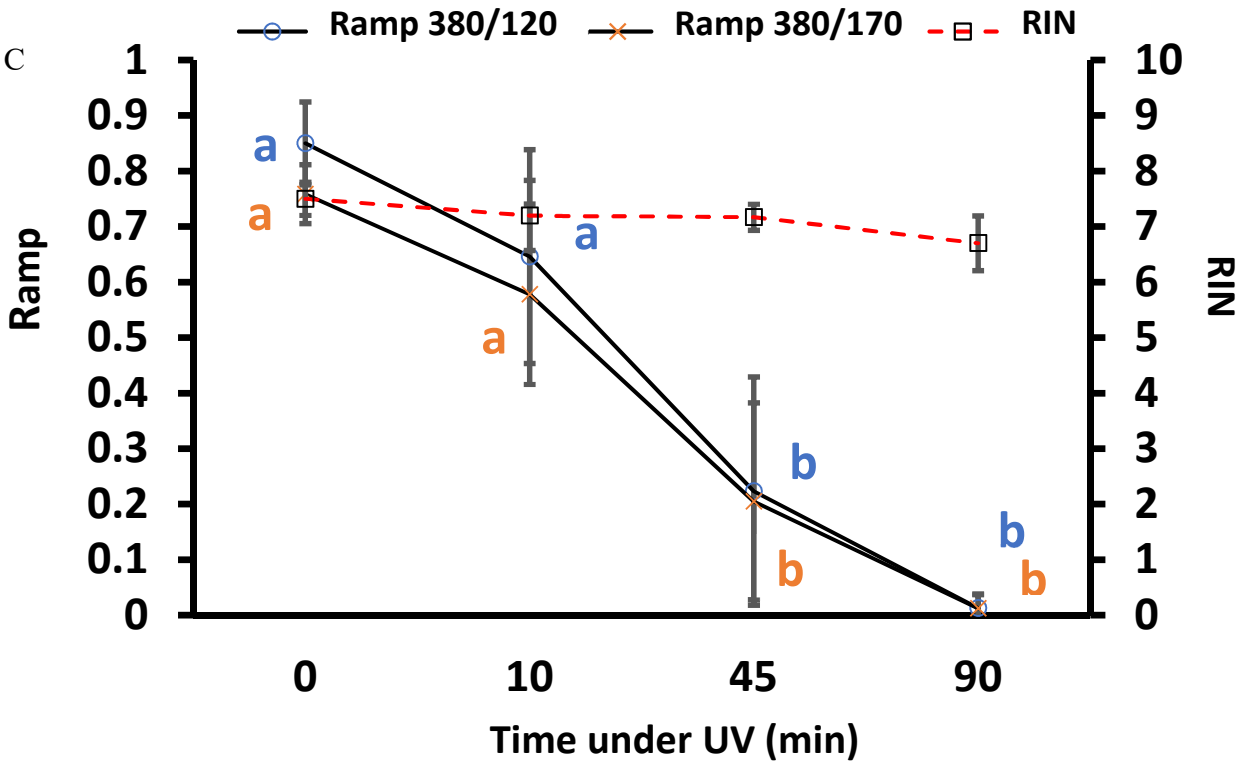

A

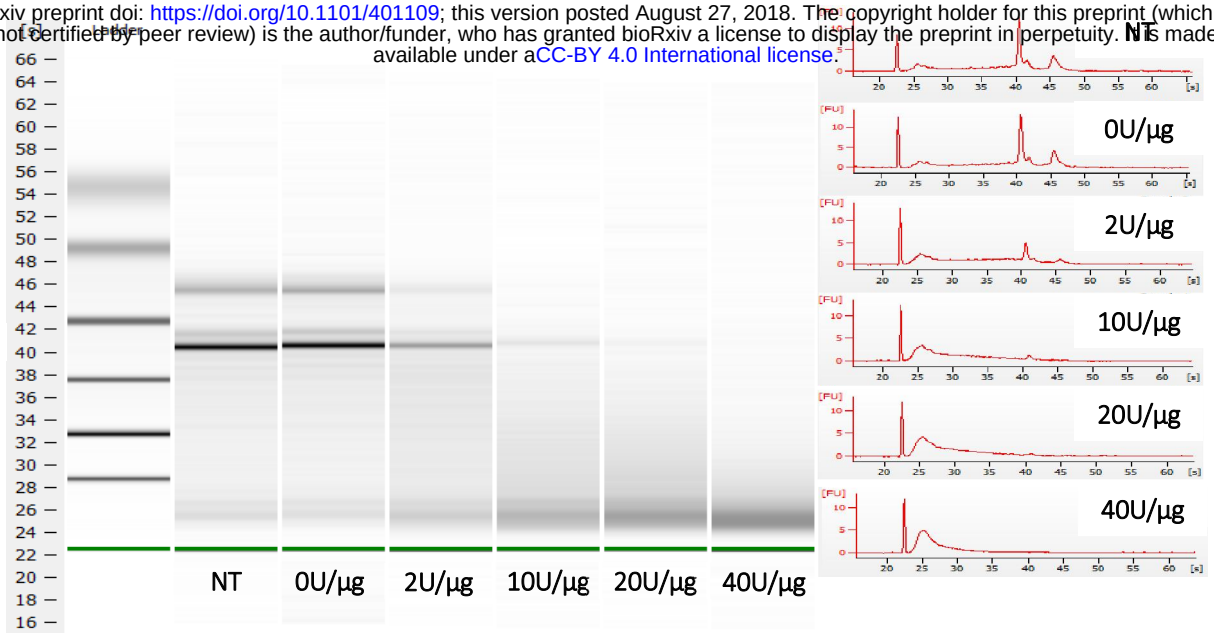

B

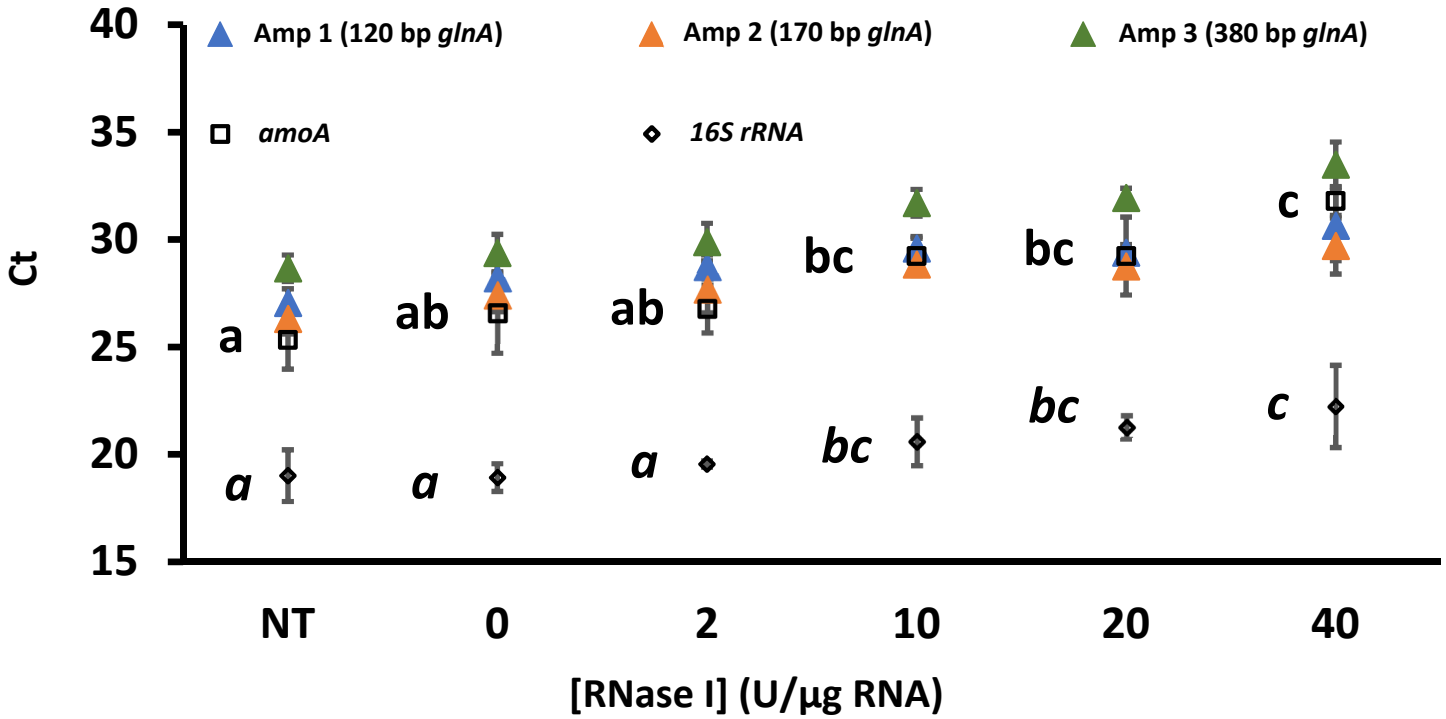

C

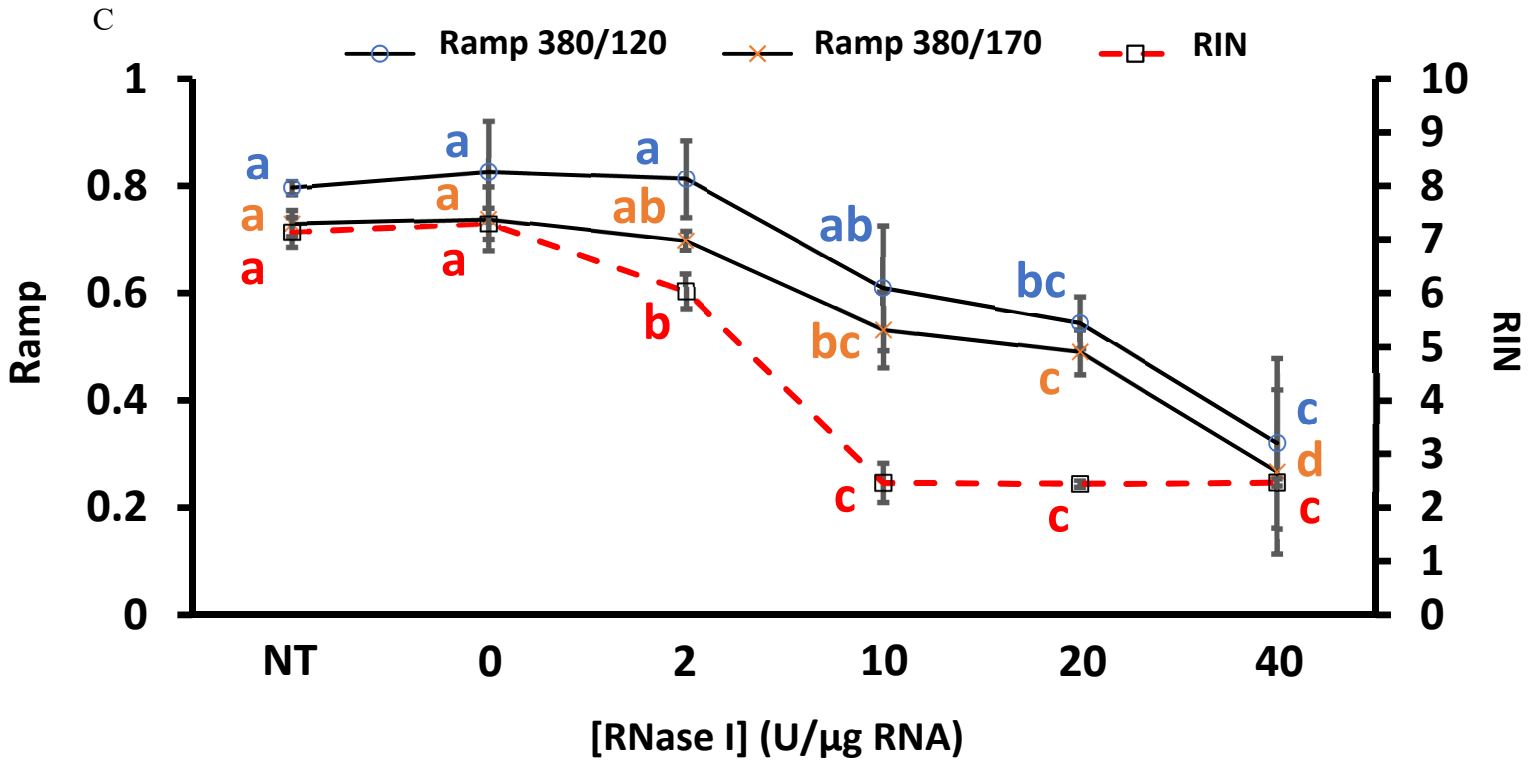

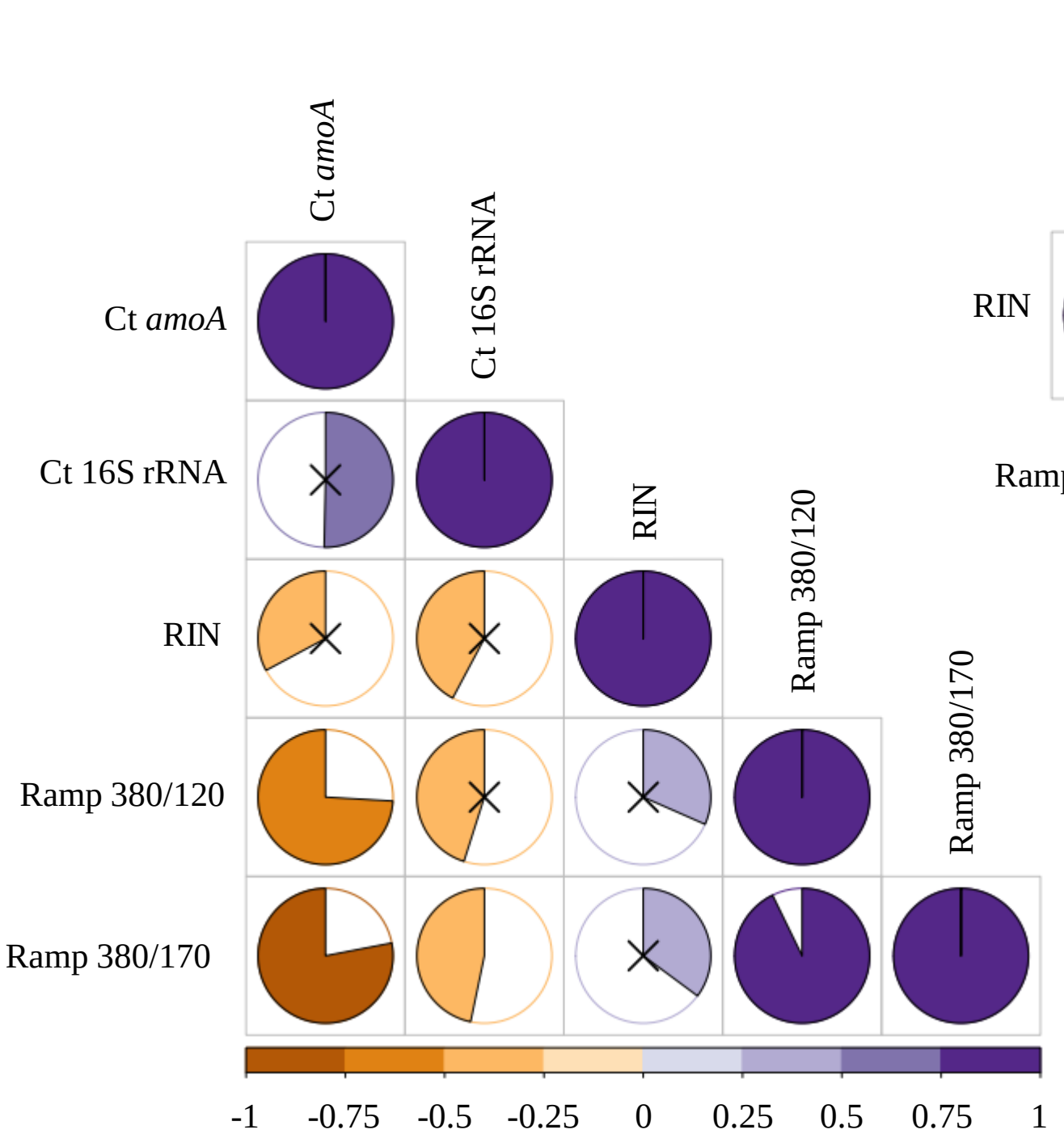
Ct amoA
Ct 16S rRNA
RIN
Ramp 380/120
Ramp 380/170
-1
-0.75
-0.5
-0.25
0
0.25
0.5
0.75
1

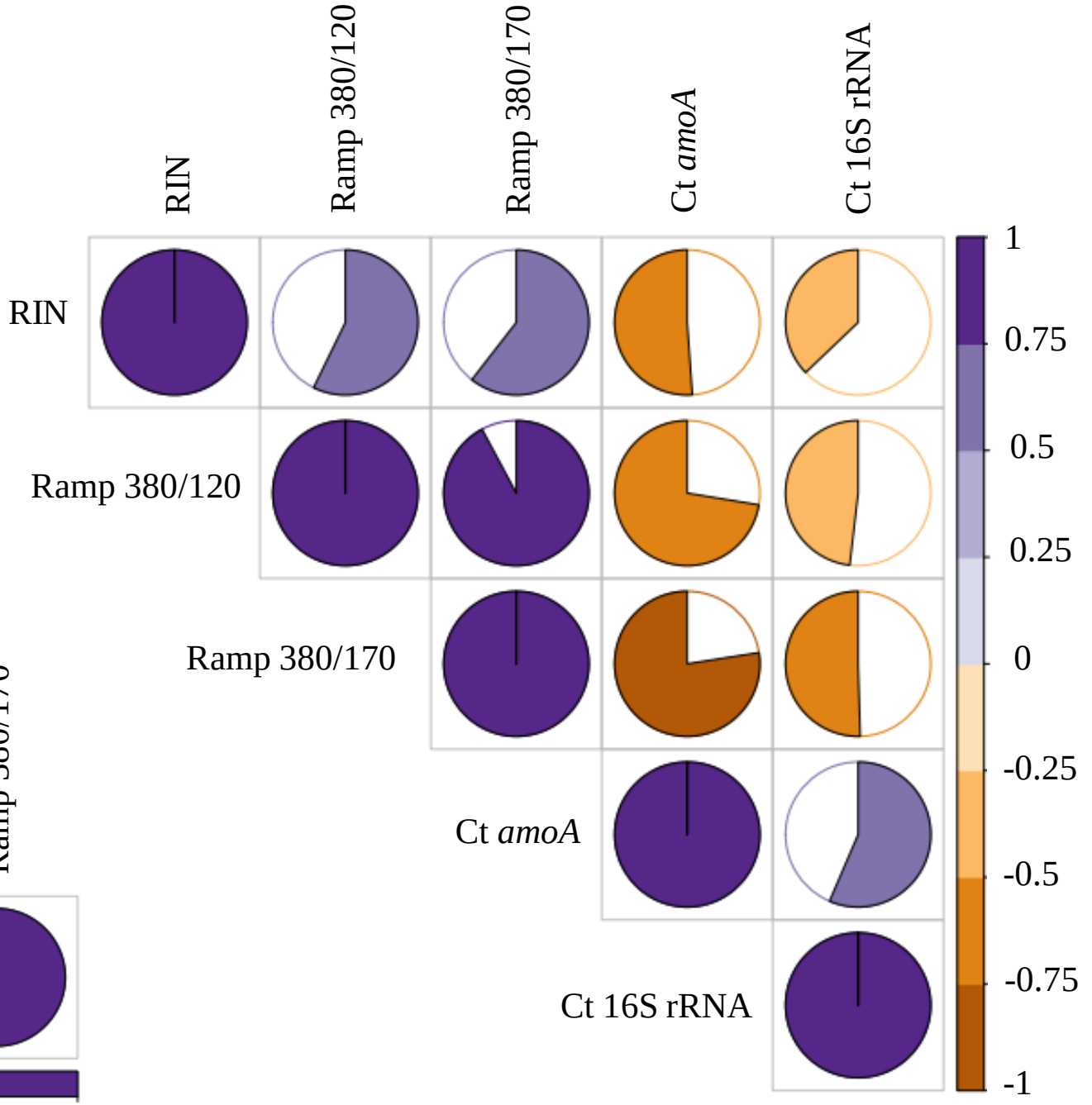
RIN
Ramp 380/120
Ramp 380/170
Ct amoA
Ct 16S rRNA
1
0.75
0.5
0.25
0
-0.25
-0.5
-0.75
-1

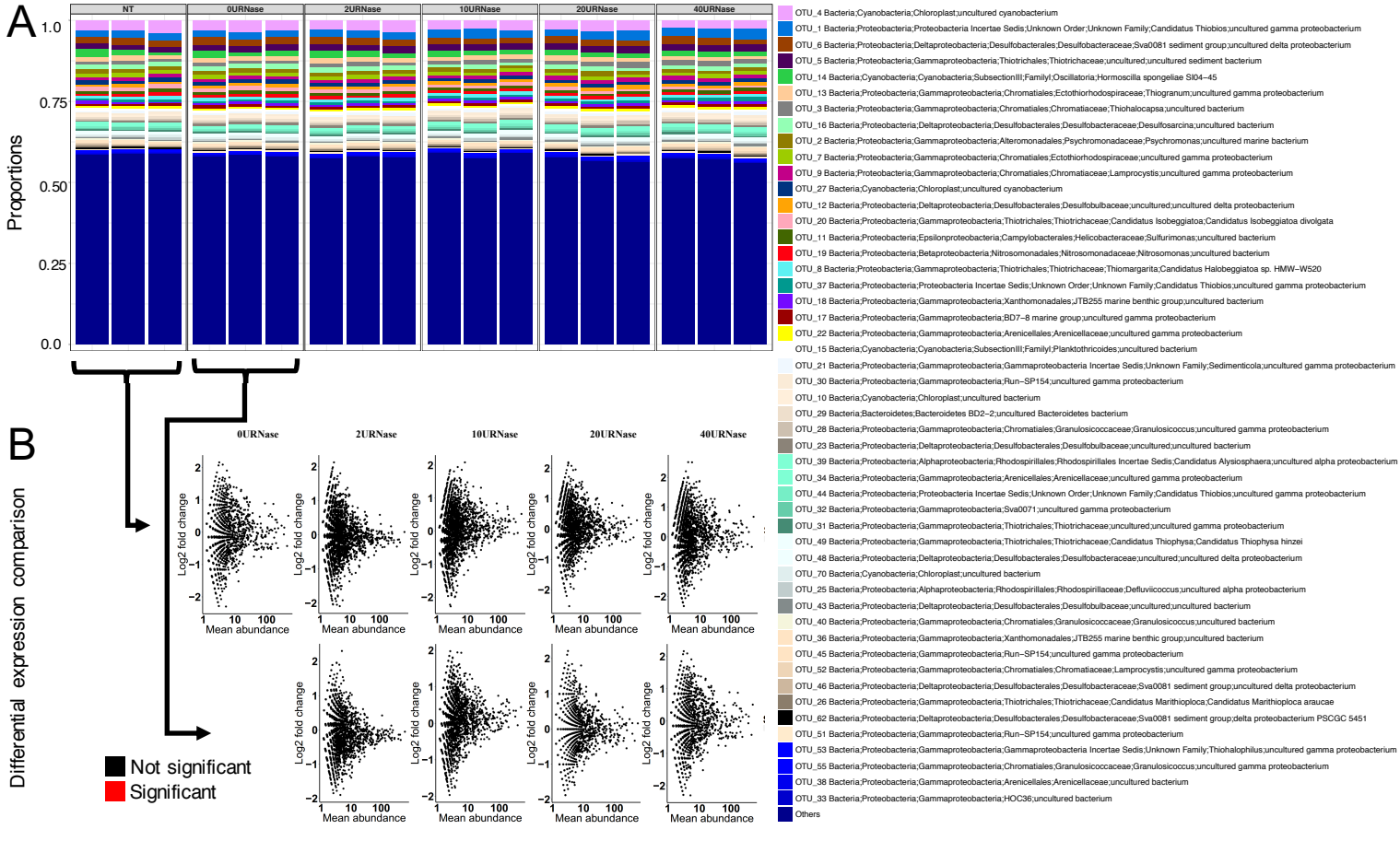
A
NT
0URNase
2URNase
10URNase
20URNase
40URNase
Proportions
1.0
0.75
0.50
0.25
0.0
OTU_4 Bacteria;Cyanobacteria;Chloroplast;uncultured cyanobacterium
OTU_1 Bacteria;Proteobacteria;Proteobacteria Incertae Sedis;Unknown Order;Unknown Family;Candidatus Thiobios;uncultured gamma proteobacterium
OTU_6 Bacteria;Proteobacteria;Deltaproteobacteria;Desulfobacterales;Desulfobacteraceae;Sva0081 sediment group;uncultured delta proteobacterium
OTU_5 Bacteria;Proteobacteria;Gammaproteobacteria;Thiotrichales;Thiotrichaceae;uncultured;uncultured sediment bacterium
OTU_14 Bacteria;Cyanobacteria;Cyanobacteria;SubsectionIII;FamilyI;Oscillatoria;Hormoscilla spongeliae SI04–45
OTU_13 Bacteria;Proteobacteria;Gammaproteobacteria;Chromatiales;Ectothiorhodospiraceae;Thiogranum;uncultured gamma proteobacterium
OTU_3 Bacteria;Proteobacteria;Gammaproteobacteria;Chromatiales;Chromatiaceae;Thiohalocapsa;uncultured bacterium
OTU_16 Bacteria;Proteobacteria;Deltaproteobacteria;Desulfobacterales;Desulfobacteraceae;Desulfosarcina;uncultured bacterium
OTU_2 Bacteria;Proteobacteria;Gammaproteobacteria;Alteromonadales;Psychromonadaceae;Psychromonas;uncultured marine bacterium
OTU_7 Bacteria;Proteobacteria;Gammaproteobacteria;Chromatiales;Ectothiorhodospiraceae;uncultured gamma proteobacterium
OTU_9 Bacteria;Proteobacteria;Gammaproteobacteria;Chromatiales;Chromatiaceae;Lamprocystis;uncultured gamma proteobacterium
OTU_27 Bacteria;Cyanobacteria;Chloroplast;uncultured cyanobacterium
OTU_12 Bacteria;Proteobacteria;Deltaproteobacteria;Desulfobacterales;Desulfobulbaceae;uncultured;uncultured delta proteobacterium
OTU_20 Bacteria;Proteobacteria;Gammaproteobacteria;Thiotrichales;Thiotrichaceae;Candidatus Isobeggiatoa;Candidatus Isobeggiatoa divolgata
OTU_11 Bacteria;Proteobacteria;Epsilonproteobacteria;Campylobacterales;Helicobacteraceae;Sulfurimonas;uncultured bacterium
OTU_19 Bacteria;Proteobacteria;Betaproteobacteria;Nitrosomonadales;Nitrosomonadaceae;Nitrosomonas;uncultured bacterium
OTU_8 Bacteria;Proteobacteria;Gammaproteobacteria;Thiotrichales;Thiotrichaceae;Thiomargarita;Candidatus Haloberggiatoa sp. HMW–W520
OTU_37 Bacteria;Proteobacteria;Proteobacteria Incertae Sedis;Unknown Order;Unknown Family;Candidatus Thiobios;uncultured gamma proteobacterium
OTU_18 Bacteria;Proteobacteria;Gammaproteobacteria;Xanthomonadales;JTB255 marine benthic group;uncultured bacterium
OTU_17 Bacteria;Proteobacteria;Gammaproteobacteria;BD7–8 marine group;uncultured gamma proteobacterium
OTU_22 Bacteria;Proteobacteria;Gammaproteobacteria;Arenicellales;Arenicellaceae;uncultured gamma proteobacterium
OTU_15 Bacteria;Cyanobacteria;Cyanobacteria;SubsectionIII;FamilyI;Planktothricoides;uncultured bacterium
OTU_21 Bacteria;Proteobacteria;Gammaproteobacteria;Gammaproteobacteria Incertae Sedis;Unknown Family;Sedimenticola;uncultured gamma proteobacterium
OTU_30 Bacteria;Proteobacteria;Gammaproteobacteria;Run–SP154;uncultured gamma proteobacterium
OTU_10 Bacteria;Cyanobacteria;Chloroplast;uncultured bacterium
OTU_29 Bacteria;Bacteroidetes;Bacteroidetes BD2–2;uncultured Bacteroidetes bacterium
OTU_28 Bacteria;Proteobacteria;Gammaproteobacteria;Chromatiales;Granulosiococcaceae;Granulosiococcus;uncultured gamma proteobacterium
OTU_23 Bacteria;Proteobacteria;Deltaproteobacteria;Desulfobacterales;Desulfobulbaceae;uncultured;uncultured bacterium
OTU_39 Bacteria;Proteobacteria;Alphaproteobacteria;Rhodospirillales;Rhodospirillales Incertae Sedis;Candidatus Alysiosphaera;uncultured alpha proteobacterium
OTU_34 Bacteria;Proteobacteria;Gammaproteobacteria;Arenicellales;Arenicellaceae;uncultured gamma proteobacterium
OTU_44 Bacteria;Proteobacteria;Proteobacteria Incertae Sedis;Unknown Order;Unknown Family;Candidatus Thiobios;uncultured gamma proteobacterium
OTU_32 Bacteria;Proteobacteria;Gammaproteobacteria;Sva0071;uncultured gamma proteobacterium
OTU_31 Bacteria;Proteobacteria;Gammaproteobacteria;Thiotrichales;Thiotrichaceae;uncultured;uncultured gamma proteobacterium
OTU_49 Bacteria;Proteobacteria;Gammaproteobacteria;Thiotrichales;Thiotrichaceae;Candidatus Thiophysa;Candidatus Thiophysa hinzei
OTU_48 Bacteria;Proteobacteria;Deltaproteobacteria;Desulfobacterales;Desulfobacteraceae;uncultured;uncultured delta proteobacterium
OTU_70 Bacteria;Cyanobacteria;Chloroplast;uncultured bacterium
OTU_25 Bacteria;Proteobacteria;Alphaproteobacteria;Rhodospirillales;Rhodospirillaceae;Defluviicoccus;uncultured alpha proteobacterium
OTU_43 Bacteria;Proteobacteria;Deltaproteobacteria;Desulfobacterales;Desulfobulbaceae;uncultured;uncultured bacterium
OTU_40 Bacteria;Proteobacteria;Gammaproteobacteria;Chromatiales;Granulosiococcaceae;Granulosiococcus;uncultured bacterium
OTU_36 Bacteria;Proteobacteria;Gammaproteobacteria;Xanthomonadales;JTB255 marine benthic group;uncultured bacterium
OTU_45 Bacteria;Proteobacteria;Gammaproteobacteria;Run–SP154;uncultured gamma proteobacterium
OTU_52 Bacteria;Proteobacteria;Gammaproteobacteria;Chromatiales;Chromatiaceae;Lamprocystis;uncultured gamma proteobacterium
OTU_46 Bacteria;Proteobacteria;Deltaproteobacteria;Desulfobacterales;Desulfobacteraceae;Sva0081 sediment group;uncultured delta proteobacterium
OTU_26 Bacteria;Proteobacteria;Gammaproteobacteria;Thiotrichales;Thiotrichaceae;Candidatus Marithioploca;Candidatus Marithioploca araucae
OTU_62 Bacteria;Proteobacteria;Deltaproteobacteria;Desulfobacterales;Desulfobacteraceae;Sva0081 sediment group;delta proteobacterium PSCGC 5451
OTU_51 Bacteria;Proteobacteria;Gammaproteobacteria;Run–SP154;uncultured gamma proteobacterium
OTU_53 Bacteria;Proteobacteria;Gammaproteobacteria;Gammaproteobacteria Incertae Sedis;Unknown Family;Thiohalophilus;uncultured gamma proteobacterium
OTU_55 Bacteria;Proteobacteria;Gammaproteobacteria;Chromatiales;Granulosiococcaceae;Granulosiococcus;uncultured gamma proteobacterium
OTU_38 Bacteria;Proteobacteria;Gammaproteobacteria;Arenicellales;Arenicellaceae;uncultured bacterium
OTU_33 Bacteria;Proteobacteria;Gammaproteobacteria;HOC36;uncultured bacterium
Others
B
Differential expression comparison
0URNase
2URNase
10URNase
20URNase
40URNase
Log2 fold change
Mean abundance
1
10
100
2
1
0
−1
−2
Not significant
Significant

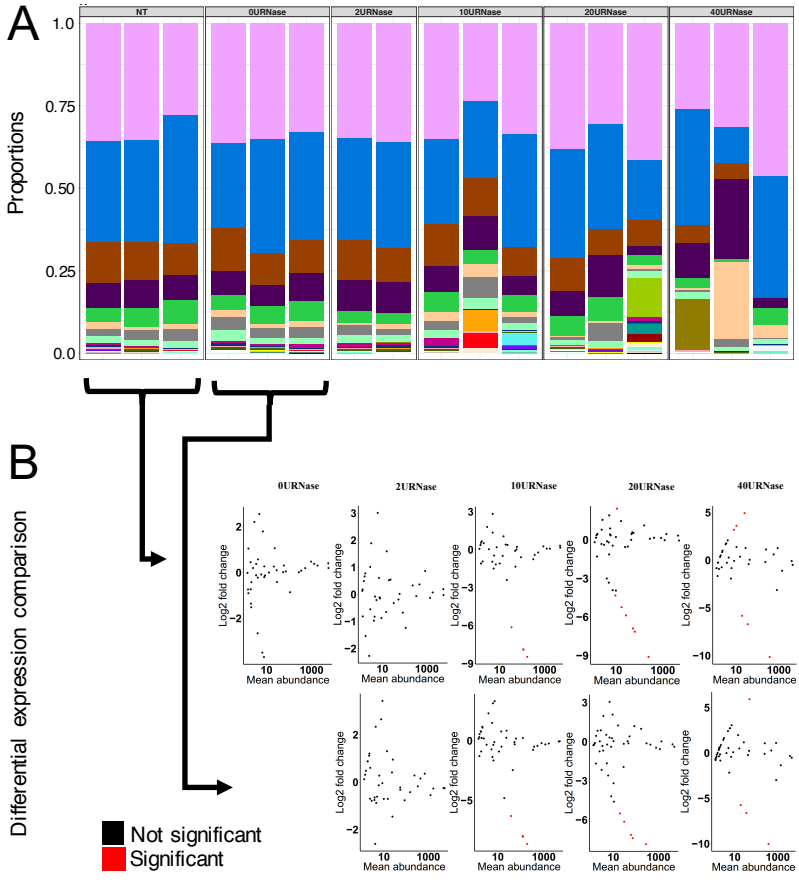

OTU_22 cellular organisms;Bacteria;Proteobacteria;Betaproteobacteria;environmental samples
OTU_4 cellular organisms;Bacteria;Proteobacteria;Betaproteobacteria;environmental samples
OTU_3 cellular organisms;Bacteria;Proteobacteria;Betaproteobacteria;environmental samples
OTU_7 cellular organisms;Bacteria;Proteobacteria;Betaproteobacteria;environmental samples
OTU_8 cellular organisms;Bacteria;Proteobacteria;Betaproteobacteria;environmental samples
OTU_2 cellular organisms;Bacteria;Proteobacteria;Betaproteobacteria;environmental samples
OTU_6 cellular organisms;Bacteria;Proteobacteria;Betaproteobacteria;environmental samples
OTU_18 cellular organisms;Bacteria;Proteobacteria;Betaproteobacteria;environmental samples
OTU_1
OTU_5
OTU_24 cellular organisms;Bacteria;environmental samples;ammonia oxidizing bacteria ensemble
OTU_13 cellular organisms;Bacteria;environmental samples
OTU_21
OTU_25 cellular organisms;Bacteria;environmental samples
OTU_19 cellular organisms;Bacteria;Proteobacteria;Betaproteobacteria;environmental samples
OTU_23
OTU_15
OTU_12
OTU_11 cellular organisms;Bacteria;Proteobacteria;Betaproteobacteria;environmental samples
OTU_9
OTU_27 cellular organisms;Bacteria;Proteobacteria;Betaproteobacteria;environmental samples
OTU_17 cellular organisms;Bacteria;Proteobacteria;Betaproteobacteria;environmental samples
OTU_44
OTU_31
OTU_33
OTU_26 cellular organisms;Bacteria;Proteobacteria;Betaproteobacteria;environmental samples
OTU_20
OTU_50 cellular organisms;Bacteria;Proteobacteria;Betaproteobacteria;environmental samples
OTU_16 cellular organisms;Bacteria;Proteobacteria;Betaproteobacteria;environmental samples
OTU_45
OTU_38
OTU_28 cellular organisms;Bacteria;Proteobacteria;Betaproteobacteria;environmental samples
OTU_46 cellular organisms;Bacteria;Proteobacteria;Betaproteobacteria;environmental samples
OTU_30
OTU_39
OTU_42 cellular organisms;Bacteria;environmental samples
OTU_10
OTU_37 cellular organisms;Bacteria;Proteobacteria;Betaproteobacteria;environmental samples
OTU_52 cellular organisms;Bacteria;Proteobacteria;Betaproteobacteria;environmental samples
OTU_41 cellular organisms;Bacteria;Proteobacteria;Betaproteobacteria;environmental samples
OTU_14
OTU_36
OTU_29 cellular organisms;Bacteria;Proteobacteria;Betaproteobacteria;environmental samples
OTU_55 cellular organisms;Bacteria;Proteobacteria;Betaproteobacteria;environmental samples
OTU_40 cellular organisms;Bacteria;Proteobacteria;Betaproteobacteria;environmental samples
OTU_43 cellular organisms;Bacteria;Proteobacteria;Betaproteobacteria;environmental samples
OTU_34
OTU_49 cellular organisms;Bacteria;Proteobacteria;Betaproteobacteria;environmental samples
OTU_32 cellular organisms;Bacteria;Proteobacteria;Betaproteobacteria;environmental samples
OTU_35 cellular organisms;Bacteria;Proteobacteria;Betaproteobacteria;environmental samples
Others

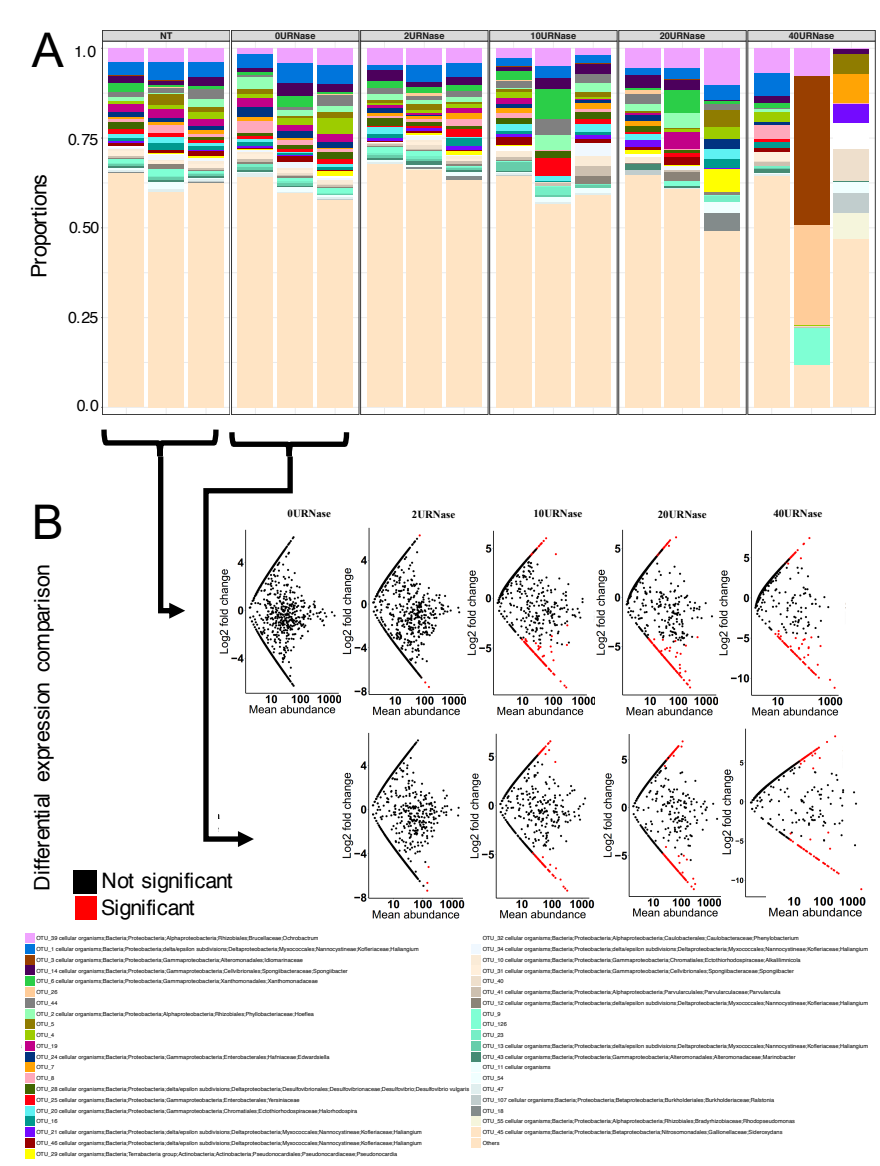
A
NT
0URNase
2URNase
10URNase
20URNase
40URNase
Proportions
1.0
0.75
0.50
0.25
0.0
B
Differential expression comparison
0URNase
2URNase
10URNase
20URNase
40URNase
Log2 fold change
Mean abundance
Not significant
Significant
OTU_39 cellular organisms;Bacteria;Proteobacteria;Alphaproteobacteria;Rhizobiales;Brucellaceae;Ochrobactrum
OTU_1 cellular organisms;Bacteria;Proteobacteria;delta/epsilon subdivisions;Deltaproteobacteria;Myxococcales;Nannocystineae;Kofleriaceae;Haliangium
OTU_3 cellular organisms;Bacteria;Proteobacteria;Gammaproteobacteria;Alteromonadales;Idiomarinaceae
OTU_14 cellular organisms;Bacteria;Proteobacteria;Gammaproteobacteria;Cellvibrionales;Spongiibacteraceae;Spongiibacter
OTU_6 cellular organisms;Bacteria;Proteobacteria;Gammaproteobacteria;Xanthomonadales;Xanthomonadaceae
OTU_26
OTU_44
OTU_2 cellular organisms;Bacteria;Proteobacteria;Alphaproteobacteria;Rhizobiales;Phyllobacteriaceae;Hoeflea
OTU_5
OTU_4
OTU_19
OTU_24 cellular organisms;Bacteria;Proteobacteria;Gammaproteobacteria;Enterobacteriales;Hafniaceae;Edwardsiella
OTU_7
OTU_8
OTU_28 cellular organisms;Bacteria;Proteobacteria;delta/epsilon subdivisions;Deltaproteobacteria;Desulfovibrionales;Desulfovibrionaceae;Desulfovibrio;Desulfovibrio vulgaris
OTU_25 cellular organisms;Bacteria;Proteobacteria;Gammaproteobacteria;Enterobacteriales;Yersiniaceae
OTU_20 cellular organisms;Bacteria;Proteobacteria;Gammaproteobacteria;Chromatiales;Ectothiorhodospiraceae;Halorhodospira
OTU_16
OTU_21 cellular organisms;Bacteria;Proteobacteria;delta/epsilon subdivisions;Deltaproteobacteria;Myxococcales;Nannocystineae;Kofleriaceae;Haliangium
OTU_45 cellular organisms;Bacteria;Proteobacteria;delta/epsilon subdivisions;Deltaproteobacteria;Myxococcales;Nannocystineae;Kofleriaceae;Haliangium
OTU_29 cellular organisms;Bacteria;Terrabacteria group;Actinobacteria;Actinobacteria;Pseudonocardiales;Pseudonocardiaceae;Pseudonocardia
OTU_32 cellular organisms;Bacteria;Proteobacteria;Alphaproteobacteria;Caulobacterales;Caulobacteraceae;Phenylobacterium
OTU_34 cellular organisms;Bacteria;Proteobacteria;delta/epsilon subdivisions;Deltaproteobacteria;Myxococcales;Nannocystineae;Kofleriaceae;Haliangium
OTU_10 cellular organisms;Bacteria;Proteobacteria;Gammaproteobacteria;Chromatiales;Ectothiorhodospiraceae;Alkalilimnicola
OTU_31 cellular organisms;Bacteria;Proteobacteria;Gammaproteobacteria;Cellvibrionales;Spongiibacteraceae;Spongiibacter
OTU_40
OTU_41 cellular organisms;Bacteria;Proteobacteria;Alphaproteobacteria;Parvularculales;Parvularculaceae;Parvularcula
OTU_12 cellular organisms;Bacteria;Proteobacteria;delta/epsilon subdivisions;Deltaproteobacteria;Myxococcales;Nannocystineae;Kofleriaceae;Haliangium
OTU_9
OTU_126
OTU_23
OTU_13 cellular organisms;Bacteria;Proteobacteria;delta/epsilon subdivisions;Deltaproteobacteria;Myxococcales;Nannocystineae;Kofleriaceae;Haliangium
OTU_43 cellular organisms;Bacteria;Proteobacteria;Gammaproteobacteria;Alteromonadales;Alteromonadaceae;Marinobacter
OTU_11 cellular organisms
OTU_54
OTU_47
OTU_107 cellular organisms;Bacteria;Proteobacteria;Betaproteobacteria;Burkholderiales;Burkholderiaceae;Ralstonia
OTU_18
OTU_55 cellular organisms;Bacteria;Proteobacteria;Alphaproteobacteria;Rhizobiales;Bradyrhizobiaceae;Rhodopseudomonas
OTU_42 cellular organisms;Bacteria;Proteobacteria;Betaproteobacteria;Nitrosomonadales;Gallionellaceae;Sideroxydans
Others